

Mathematical Foundations of Regular Quantum Graphs

R. Blümel, Yu. Dabaghian and R. V. Jensen

Department of Physics, Wesleyan University, Middletown, CT 06459-0155

(November 4, 2018)

Abstract

We define a class of quantum systems called regular quantum graphs. Although their dynamics is chaotic in the classical limit with positive topological entropy, the spectrum of regular quantum graphs is explicitly computable analytically and exactly, state by state, by means of periodic orbit expansions. We prove analytically that the periodic orbit series exist and converge to the correct spectral eigenvalues. We investigate the convergence properties of the periodic orbit series and prove rigorously that both conditionally convergent and absolutely convergent cases can be found. We compare the periodic orbit expansion technique with Lagrange's inversion formula. While both methods work and yield exact results, the periodic orbit expansion technique has conceptual value since all the terms in the expansion have direct physical meaning and higher order corrections are obtained according to physically obvious rules. In addition our periodic orbit expansions provide explicit analytical solutions for many classic text-book examples of quantum mechanics that previously could only be solved using graphical or numerical techniques.

03.65.Ge,02.30.Lt

arXiv:quant-ph/0203126v1 25 Mar 2002

I. INTRODUCTION

At a first glance it may seem surprising that many chaotic dynamical systems have explicit analytical solutions. But many examples are readily at hand. The shift map [1,2]

$$x_{n+1} = (2x_n) \bmod 1, \quad x_n \in \mathbf{R}, \quad n = 0, 1, 2, \dots, \quad (1.1)$$

for instance, is “Bernoulli” [2], the strongest form of chaos. Nevertheless the shift map is readily solved explicitly,

$$x_n = (2^n x_0) \bmod 1, \quad x_n \in \mathbf{R}, \quad n = 0, 1, 2, \dots \quad (1.2)$$

Another example is provided by the logistic mapping

$$x_{n+1} = \mu x_n(1 - x_n), \quad x_n \in [0, 1], \quad 0 \leq \mu \leq 4, \quad n = 0, 1, 2, \dots, \quad (1.3)$$

widely used in population dynamics [1–3]. For $\mu = 4$ this mapping is equivalent with the shift map [4] and therefore again completely chaotic. Yet an explicit solution, valid at $\mu = 4$, is given by [4,5]:

$$x_n = \sin^2(2^n \arcsin \sqrt{x_0}), \quad x_0 \in [0, 1]. \quad (1.4)$$

Therefore, as far as classical chaos is concerned, there is no basis for the belief that classically chaotic systems do not allow for explicit analytical solutions. But what about the quantized versions of classically chaotic systems, commonly known as quantum chaotic systems [6,7]? Here, too, the answer is affirmative. It was shown recently [8–12] that regular quantum graphs provide a large class of explicitly solvable quantum chaotic systems. In order to strengthen first analytical and numerical results presented in [8–12], it is the purpose of this paper to show that the explicit periodic orbit expansions obtained in [8–12] are more than formal identities. We will prove below that (i) the spectrum of regular quantum graphs is computable explicitly and analytically, state by state, via convergent periodic orbit expansions and (ii) the periodic orbit series converge to the correct spectral eigenvalues.

The main body of this paper is organized as follows. In Sec. II we summarize the basics of quantum graph theory and derive the general form of the spectral equation. In Sec. III we define regular quantum graphs. In Sec. IV we present the explicit periodic orbit expansions of individual eigenvalues of regular quantum graphs. We also specify a summation scheme that guarantees convergence to the correct results. The derivations presented in Sec. IV are mathematically rigorous except for one step where we interchange integration and summation to arrive at our final results. This is a “dangerous operation”, which is not allowed without further investigation. This point is resolved in Sec. V, where we present the analytical proofs that justify the interchange of integration and summation performed in Sec. IV. This result establishes that the periodic orbit expansions investigated in this paper converge in the usual sense of elementary analysis. In Sec. VI we investigate the convergence properties of the periodic orbit series obtained in Sec. IV. We prove analytically that there exists at least one quantum graph for which the convergence is not absolute, but conditional. According to Riemann’s well-known reordering theorem (see, e.g. [13], volume II, page 33), it is possible to reorder the terms of a conditionally convergent sum in such a way that it converges to any prescribed number. This is the reason why in Sec. IV we place so much emphasis on specifying a summation scheme that guarantees convergence of the periodic orbit sums to the correct spectral eigenvalues. In Sec. VII we present an alternative way of solving the spectral equations of regular quantum graphs: Lagrange’s inversion formula. Although a perfectly sound and fast-converging method for solving the spectral equation, it lacks the physical appeal of periodic orbit expansions which are based on concrete physical objects such as periodic orbits and their geometrical and dynamical properties. In Sec. VIII we discuss our results, point out promising research directions and conclude the paper.

Since many scientists will find the existence of convergent periodic orbit expansions surprising, we found it necessary to establish this result with an extra degree of rigor. This necessarily requires strong, but somewhat technical proofs. However, in order not to break the flow of the paper, we adopt a hierarchical approach presenting the material in three

stages. The most pertinent aspects of our results are presented in the main text as outlined above. Supporting higher-level, but formal, material is presented in Appendix A. Lower level material, such as formulae, definitions and lemmas, is relegated to Appendix B.

In order for the proofs to be convincing, and to be accessible to a wide readership, we used only concepts of elementary undergraduate analysis in our proofs, altogether avoiding advanced mathematical concepts, such as distributions [14,15]. This is an important point since our paper seeks mathematical rigor on a common basis acceptable to all readers. In this spirit the alert reader will notice that we completely avoid the use of Dirac’s delta “function” [16]. This is necessary since the delta “function” is a distribution [14,15], a concept we found to be highly confusing for the general reader. Although there is nothing “wrong” with the delta “function”, if treated properly as a distribution or linear functional, the confusion surrounding the delta “function” started with von Neumann’s critique [17] at a time when the modern tools of distribution theory were not yet available. Therefore, although ultimately completely unjustified, von Neumann’s critique [17] tainted the delta “function” to such an extent that it still can’t be used in a rigorous context without causing heated debate. Thus, for the sake of simplicity and clarity of our arguments, we prefer to avoid it. As a consequence, the presentation of the material in this paper and all of our proofs are conducted without using the concept of level densities, which are usually defined with the help of Dirac’s delta “function”.

We emphasize that there is a fundamental difference between an analytical solution and an *explicit* analytical solution. While the spectral equation for quantum graphs is known in great detail [18], and periodic orbit expansions for the spectral density and the staircase function of quantum graphs are known [18], these results are all implicit. This means that they do not yield the spectral eigenvalues in the form “ $E_n = \dots$ ”. It is the novelty of this paper to obtain explicit analytical expressions of this type for a wide class of quantum chaotic systems, and prove their validity and convergence with mathematical rigor.

II. QUANTUM GRAPHS AND SPECTRAL EQUATION

The properties of the Laplacian operator on graphs have been studied in great detail in the mathematical literature [19,20] and the study of quantum mechanics on graphs has attracted considerable attention among chemists and physicists (see, e.g., [21–23] and references therein), especially in the quantum chaos community [18,22,24–27]. The purpose of this section is to acquaint the reader with the main ideas of quantum graph theory. Since many excellent publications on the theory of quantum graphs are available (see, e.g., [18,22–27]), we will present only those ideas and facts that are of direct relevance to the subject of this paper.

A quantum graph consists of a network of bonds and vertices with a quantum particle travelling on it. An example of a graph with ten bonds and six vertices is shown in Fig. 1. The number of bonds is denoted by N_B , the number of vertices by N_V . In this paper we focus entirely on finite quantum graphs, i.e. $N_B, N_V < \infty$. We define directed bonds on the graph such that the bond B_{ij} connecting vertex number i with vertex number j is different from the bond B_{ji} connecting the vertices in the opposite direction. There are $2N_B$ directed bonds. It is useful to define the linearized bond index $\Lambda = 1, \dots, N_B: (ij) \mapsto \Lambda, i < j, i$ and j connected. The index Λ labels sequentially all N_B directed bonds of the graph with $i < j$. For the directed bonds B_{ij} with $i > j$ we define $\Lambda(ij) = -\Lambda(ji)$. This way the sign of the counting index reflects the directionality of the bond. The network of bonds and vertices defines the graph's topology. The topology of a graph alone does not completely specify the quantum graph. This is so because, for instance, the bonds of the graph may be dressed with potentials [9]. Since the quantum graphs we study in this paper are finite, bounded systems, their spectra are discrete.

The spectrum of a quantum graph is obtained by solving the one-dimensional Schrödinger equation on the graph subjected to the usual boundary conditions of continuity and quantum flux conservation. A particularly useful way of obtaining the spectral equation for a given quantum graph is the scattering quantization approach [18,24,28] which yields the spectral

equation in the form

$$\det[1 - S(k)] = 0, \quad (2.1)$$

where S is the quantum scattering matrix of the graph [18,22,24] and k is the wave number, related to the energy via $E = k^2$. For our purposes it is sufficient to know that the S matrix is of dimension $2N_B \times 2N_B$ and can be decomposed into [12,18]

$$S(k) = D(k)U(k), \quad (2.2)$$

where $U(k)$ is a $2N_B \times 2N_B$ unitary matrix and $D(k)$ is a diagonal matrix of the form

$$D_{\Lambda,\Lambda'}(k) = \exp[iL_{\Lambda}(k)] \delta_{\Lambda,\Lambda'}, \quad \Lambda, \Lambda' = \pm 1, \dots, \pm N_B \quad (2.3)$$

with $L_{\Lambda}(k) \in \mathbf{R}$, $L_{\Lambda}(k) = L_{-\Lambda}(k) > 0$. The ordering of the matrices D and U in (2.2) is neither unique nor important in the present context. It depends on the details of how “in” and “out” channels are assigned to the indices of the S matrix. Since the computation of the energy spectrum involves only traces and determinants, the precise ordering of D and U in (2.2) does not affect our final results.

Physically the quantities $L_{\Lambda}(k)$ are the time-reversal invariant parts of the bond actions [10,12,18]. A possible time-reversal breaking part of the bond actions is understood to be absorbed in the matrix U [12]. For simplicity we will in the following refer to L_{Λ} as the bond action of the bond B_{Λ} .

In this paper we focus exclusively on scaling quantum graphs [8–12,29]. In this case the matrix U is a constant matrix, independent of k , and the actions $L_{\Lambda}(k)$ in (2.3) split into the product $L_{\Lambda}(k) = L_{\Lambda}^{(0)}k$, where $L_{\Lambda}^{(0)} \in \mathbf{R}$ is a constant, the reduced bond action of the bond B_{Λ} . Physically the scaling case is an important case since it describes systems free from phase-space metamorphoses [30]. Scaling systems of this type arise in many physical contexts, for instance in microwave cavities partially filled with a dielectric [31–33], or Rydberg atoms in external fields [34].

It is possible to write (2.1) as a linear combination of trigonometric functions whose frequencies are directly related to the bond actions. In order to derive this representation we start by noting that

$$\det[1 - S] = \det(S^{1/2}) (-4)^{N_B} \prod_{l=1}^{2N_B} \sin(\sigma_l/2), \quad (2.4)$$

where $\sigma_l \in \mathbf{R}$ are the eigenphases of the unitary matrix S . From (2.4) we obtain the important result that

$$\det(S^{-1/2}) \det[1 - S] \in \mathbf{R}. \quad (2.5)$$

According to (2.2) we have

$$\det(S^{-1/2}) = \exp(-i\tau/2) \exp\left(-i \sum_{\Lambda=1}^{N_B} L_{\Lambda}^{(0)} k\right), \quad (2.6)$$

where τ is the eigenphase of the unitary matrix U , i.e. $\det(U) = \exp(i\tau)$. Using the decomposition (2.2) of the S matrix we write the spectral determinant (2.1) in the form

$$\det[(-U^{-1}) + D] = 0, \quad (2.7)$$

so that we can directly apply the results in Ref. [35]. According to Ref. [35], p. 87, the determinant (2.7) is a polynomial in the $2N_B$ variables $\exp(iL_{\Lambda}^{(0)} k)$, $\Lambda = \pm 1, \dots, \pm N_B$, whose coefficients are the principal sub-determinants [35] of $-U^{-1}$. Using $L_{-\Lambda}^{(0)} = L_{\Lambda}^{(0)}$ together with the fact that $\det(U^{-1})$ is the principal sub-determinant of $-U^{-1}$ of order zero [35], we obtain that (2.7) is of the form

$$\det[(-U^{-1}) + D] = \det(U^{-1}) + \sum_{n=1}^{N_B} \sum_{i_1, \dots, i_n} \sum_{\alpha^{(n)}} A_{n; i_1, \dots, i_n; \alpha^{(n)}} \exp\left[i \sum_{\Lambda \in \{i_1, \dots, i_n\}} \alpha_{\Lambda}^{(n)} L_{\Lambda}^{(0)} k\right], \quad (2.8)$$

where $1 \leq i_1 < i_2 < \dots < i_n \leq N_B$, $\alpha^{(n)}$ is an integer array of length n containing a “1,2-pattern”, i.e. $\alpha_{\Lambda}^{(n)} \in \{1, 2\}$, and $A_{n; i_1, \dots, i_n; \alpha^{(n)}}$ are complex coefficients that can be computed from the principal sub-determinants of $-U^{-1}$. Because of (2.5), we have

$$\det(S^{-1/2}) \det(U) \det(-U^{-1} + D) \in \mathbf{R}. \quad (2.9)$$

Defining

$$\omega_0 = \sum_{\Lambda=1}^{N_B} L_{\Lambda}^{(0)} \quad (2.10)$$

and using (2.6) and (2.8), we obtain (2.9) in the form

$$\exp[-i(\omega_0 k + \tau/2)] + \sum_{n=1}^{N_B} \sum_{i_1, \dots, i_n} \sum_{\alpha^{(n)}} A_{n; i_1, \dots, i_n; \alpha^{(n)}} \exp\{-i[\beta_{n; i_1, \dots, i_n; \alpha^{(n)}} k - \tau/2]\} \in \mathbf{R}, \quad (2.11)$$

where

$$\beta_{n; i_1, \dots, i_n; \alpha^{(n)}} = \omega_0 - \sum_{\Lambda \in \{i_1, \dots, i_n\}} \alpha_{\Lambda}^{(n)} L_{\Lambda}^{(0)}. \quad (2.12)$$

We define the frequencies

$$\omega_{n; i_1, \dots, i_n; \alpha^{(n)}} = |\beta_{n; i_1, \dots, i_n; \alpha^{(n)}}|. \quad (2.13)$$

Because of $L_{\Lambda}^{(0)} > 0$ for all Λ and the structure of $\alpha^{(n)}$, the largest frequency in (2.13) is ω_0 defined in (2.10). We now scan the frequencies $\omega_{n; i_1, \dots, i_n; \alpha^{(n)}}$ defined in (2.13) and collect the pairwise different ones into a set $\Omega = \{\omega_0, \dots, \omega_M\}$, where $M + 1 = |\Omega|$ is the number of pairwise different frequencies and $\omega_M < \omega_{M-1} < \dots < \omega_0$. Since the derivation of (2.11) involved only factoring nonzero terms out of the left-hand side of (2.1), the zeros of (2.11) and the zeros of (2.1) are identical. Taking the real part of the real quantity (2.11) shows that (2.1) can be written in the form

$$\cos(\omega_0 k - \pi\gamma_0) - \tilde{\Phi}(k) = 0, \quad (2.14)$$

where

$$\tilde{\Phi}(k) = \sum_{i=1}^M a_i \cos(\omega_i k - \pi\gamma_i) \quad (2.15)$$

and $a_i, \gamma_i, i = 0, \dots, M$ are real constants. In general it is difficult to obtain an explicit analytical result for the zeros of (2.14). There is, however, a subset of quantum graphs defined in the following section, that allows us to compute an explicit analytical solution of (2.14).

III. REGULAR QUANTUM GRAPHS

A subset of quantum graphs are regular quantum graphs. They fulfil the condition

$$\alpha = \sum_i |a_i| < 1, \quad (3.1)$$

where the constants a_i are the coefficients of the trigonometric functions in (2.15). Although regular quantum graphs are a restricted sub-set of all quantum graphs, they are still quantum chaotic with positive topological entropy [8,10–12]. Because of (3.1) we have $|\tilde{\Phi}(k)| < 1$ for all k , and the zeros k_n of (2.14) are given by:

$$k_n = \bar{k}_n + \tilde{k}_n, \quad n = 1, 2, \dots, \quad (3.2)$$

where

$$\bar{k}_n = \frac{\pi}{\omega_0} \left[n + \mu + \frac{1}{2} + \gamma_0 \right] \quad (3.3)$$

and

$$\tilde{k}_n = \frac{(-1)^{n+\mu}}{\omega_0} \left[\arccos[\tilde{\Phi}(k_n)] - \frac{\pi}{2} \right] \quad (3.4)$$

may be interpreted as the average and fluctuating parts of the zeros of (2.14), respectively. Since (2.14) is the spectral equation of a physics problem, we only need to study the positive solutions of (2.14). Therefore we introduced the constant $\mu \in \mathbf{Z}$ in (3.3) which allows us to adjust the counting scheme of zeros in such a way that k_1 is the first nonnegative solution of (2.14). This is merely a matter of convenience and certainly not a restriction of generality. Because of (3.1), the boundedness of the trigonometric functions in (2.15) and the properties of the arccos function, the fluctuating part of the zeros is bounded. We have

$$|\tilde{k}_n| \leq \tilde{k}_{\max} := \frac{1}{\omega_0} \left[\frac{\pi}{2} - \arccos(\alpha) \right] < \frac{\pi}{2\omega_0}. \quad (3.5)$$

Therefore, roots of (2.14) can only be found in the intervals $R_n = [\bar{k}_n - \tilde{k}_{\max}, \bar{k}_n + \tilde{k}_{\max}]$.

We define

$$\hat{k}_n = \frac{\pi}{\omega_0}(n + \mu + 1 + \gamma_0), \quad n = 1, 2, \dots \quad (3.6)$$

and note in passing that

$$\bar{k}_n = (\hat{k}_{n-1} + \hat{k}_n)/2. \quad (3.7)$$

We also define the open interval $I_n = (\hat{k}_{n-1}, \hat{k}_n)$ and its closure $\bar{I}_n = [\hat{k}_{n-1}, \hat{k}_n]$. For $\alpha < 1$ we have $R_n \subset I_n$. For $\alpha \rightarrow 1$ the root intervals R_n grow in size towards I_n , but for any $\alpha < 1$ the end points \hat{k}_{n-1} and \hat{k}_n of \bar{I}_n are not roots of (2.14). The boundedness of \tilde{k}_n also implies the existence of two root-free intervals in I_n . They are given by $F_n^{(-)} = [\hat{k}_{n-1}, \bar{k}_n - \tilde{k}_{\max}]$ and $F_n^{(+)} = [\bar{k}_n + \tilde{k}_{\max}, \hat{k}_n]$. Thus, roots cannot be found in the union of these two intervals, the root-free zone $F_n = F_n^{(-)} \cup F_n^{(+)} \subset \bar{I}_n$. We also have $\bar{I}_n = F_n \cup R_n$. For an illustration of the various intervals defined above, and their relation to each other, see Fig. 2. The intervals I_n together with their limiting points \hat{k}_n provide a natural organization of the k axis into a periodic structure of root cells.

We now define $x = \omega_0 k - \pi\gamma_0$, which transforms (2.14) into

$$\cos(x) - \Phi(x) = 0, \quad \Phi(x) = \sum_{i=1}^M a_i \cos(\rho_i x - \pi\nu_i), \quad (3.8)$$

where $\rho_i = \omega_i/\omega_0$ and $\nu_i = \gamma_i - \rho_i\gamma_0$. Since, as discussed in Sec. II, ω_0 is the largest frequency in (2.14), we have $\rho_i < 1$, $i = 1, \dots, M$, and theorem T2 (Appendix A) is applicable. It states that there is exactly one zero x_n of (3.8) in every open interval $(n\pi, (n+1)\pi)$, $n \in \mathbf{Z}$. Consulting Fig. 3 this fact is intuitively clear since the \cos function in (3.8) is “fast”, and $\Phi(x)$, containing only frequencies smaller than 1, is a “slow” function. Thus, as illustrated in Fig. 3, and proved rigorously by T2 (Appendix A), there is one and only one intersection between the fast \cos function and the slow Φ function in every x interval of length π . Transformed back to the variable k this implies that there is exactly one zero k_n of (2.14) in every interval I_n . Since this zero cannot be found in the root-free zone F_n , it has to be located in R_n . Thus there is exactly one root k_n of (2.14) in every root-interval R_n . This fact is the key for obtaining explicit analytical solutions of (2.14) as discussed in the following section.

IV. PERIODIC ORBIT EXPANSIONS FOR INDIVIDUAL SPECTRAL POINTS

For the zeros of (2.14) we define the spectral staircase

$$N(k) = \sum_{i=1}^{\infty} \theta(k - k_i), \quad (4.1)$$

where

$$\theta(x) = \begin{cases} 0, & \text{for } x < 0, \\ 1/2, & \text{for } x = 0, \\ 1, & \text{for } x > 0, x \in \mathbf{R} \end{cases} \quad (4.2)$$

is Heavyside's θ function. Based on the scattering quantization approach it was shown elsewhere [18] that

$$N(k) = \bar{N}(k) + \frac{1}{\pi} \text{Im Tr} \sum_{l=1}^{\infty} \frac{1}{l} S^l(k), \quad (4.3)$$

where

$$\bar{N}(k) = \frac{\omega_0 k}{\pi} - (\mu + 1 + \gamma_0), \quad (4.4)$$

and $S(k)$ is the unitary scattering matrix (2.2) of the quantum graph. Since, according to our assumptions, S is a finite, unitary matrix, existence and convergence of (4.3) is guaranteed according to L17, L18 and L19 (Appendix B). Therefore, $N(k)$ is well-defined for all k . Since $S(k)$ can easily be constructed for any given quantum graph [12,18], (4.3) provides an explicit formula for the staircase function (4.1). Combined with the spectral properties of regular quantum graphs discussed in Sec. III, this expression now enables us to explicitly compute the zeros of (2.14).

In Sec. III we proved that exactly one zero k_n of (2.14) is located in $I_n = (\hat{k}_{n-1}, \hat{k}_n)$. Integrating $N(k)$ from \hat{k}_{n-1} to \hat{k}_n and taking into account that $N(k)$ jumps by one unit at $k = k_n$ (see illustration in Fig. 4), we obtain

$$\int_{\hat{k}_{n-1}}^{\hat{k}_n} N(k) dk = N(\hat{k}_{n-1})[k_n - \hat{k}_{n-1}] + N(\hat{k}_n)[\hat{k}_n - k_n]. \quad (4.5)$$

Solving for k_n and using $N(\hat{k}_{n-1}) = n - 1$ and $N(\hat{k}_n) = n$ (see Fig. 4), we obtain

$$k_n = \frac{\pi}{\omega_0} (2n + \mu + \gamma_0) - \int_{\bar{k}_{n-1}}^{\bar{k}_n} N(k) dk. \quad (4.6)$$

Since we know $N(k)$ explicitly, (4.6) allows us to compute every zero of (2.14) explicitly and individually for any choice of n . The representation (4.6) requires no further proof since, as mentioned above, $N(k)$ is well-defined everywhere, and is Riemann-integrable over any finite interval of k .

Another useful representation of k_n is obtained by substituting (4.3) with (4.4) into (4.6) and using (3.3):

$$k_n = \bar{k}_n - \frac{1}{\pi} \text{Im Tr} \int_{\bar{k}_{n-1}}^{\bar{k}_n} \sum_{l=1}^{\infty} \frac{1}{l} S^l(k) dk. \quad (4.7)$$

According to theorem T3 (Appendix A) presented in Sec. V, it is possible to interchange integration and summation in (4.7) and we arrive at

$$k_n = \bar{k}_n - \frac{1}{\pi} \text{Im Tr} \sum_{l=1}^{\infty} \frac{1}{l} \int_{\bar{k}_{n-1}}^{\bar{k}_n} S^l(k) dk. \quad (4.8)$$

In many cases the integral over $S^l(k)$ can be performed explicitly, which yields explicit representations for k_n .

Finally we discuss explicit representations of k_n in terms of periodic orbits. Based on the product form (2.2) of the S matrix and the explicit representation (2.3) of the matrix elements of D , the trace of $S(k)^l$ is of the form

$$\text{Tr} S(k)^l = \sum_{j_1 \dots j_l} D_{j_1, j_1} U_{j_1, j_2} D_{j_2, j_2} U_{j_2, j_3} \dots D_{j_l, j_l} U_{j_l, j_1} = \sum_{m \in P[l]} A_m[l] \exp \{ i L_m^{(0)}[l] k \}, \quad (4.9)$$

where $P[l]$ is the index set of all possible periodic orbits of length l of the graph, $A_m[l] \in \mathbf{C}$ is the weight of orbit number m of length l , computable from the matrix elements of U , and $L_m^{(0)}[l]$ is the reduced action of periodic orbit number m of length l . Using this result together with (3.7) we obtain the explicit periodic orbit formula for the spectrum in the form

$$k_n = \bar{k}_n - \frac{2}{\pi} \text{Im} \sum_{l=1}^{\infty} \frac{1}{l} \sum_{m \in P[l]} A_m[l] \frac{e^{i L_m^{(0)}[l] \bar{k}_n}}{L_m^{(0)}[l]} \sin \left[\frac{\pi}{2\omega_0} L_m^{(0)}[l] \right]. \quad (4.10)$$

Since the derivation of (4.10) involves only a resummation of $\text{Tr } S^l$ (which involves only a finite number of terms), the convergence properties of (4.8) are unaffected, and (4.10) converges.

Reviewing our logic that took us from (4.6) to (4.10) it is important to stress that (4.10) converges to the correct result for k_n . This is so because starting from (4.6), which we proved to be exact, we arrive at (4.10) performing only allowed equivalence transformations (as mentioned already, the step from (4.7) to (4.8) is proved in Sec. V). This is an important result. It means that even though (4.10) may be a series that converges only conditionally (in Sec. VI we prove that this is indeed the case for at least one quantum graph), it still converges to the correct result, provided the series is summed exactly as specified in (4.10). The summation scheme specified in (4.10) means that periodic orbits have to be summed according to their symbolic lengths (see, e.g., [1,2,5,6,29]) and not, e.g., according to their action lengths. If this proviso is properly taken into account, (4.10) is an explicit, convergent periodic orbit representation for k_n that converges to the exact value of k_n .

It is possible to re-write (4.10) into the more familiar form of summation over prime periodic orbits and their repetitions. Any periodic orbit m of length l in (4.10) consists of an irreducible, prime periodic orbit $m_{\mathcal{P}}$ of length $l_{\mathcal{P}}$ which is repeated ν times, such that

$$l = \nu l_{\mathcal{P}}. \quad (4.11)$$

Of course ν may be equal to 1 if orbit number m is already a prime periodic orbit. Let us now focus on the amplitude $A_m[l]$ in (4.8). If we denote by $A_{m_{\mathcal{P}}}$ the amplitude of the prime periodic orbit, then

$$A_m[l] = l_{\mathcal{P}} A_{m_{\mathcal{P}}}^{\nu}. \quad (4.12)$$

This is so, because the prime periodic orbit $m_{\mathcal{P}}$ is repeated ν times, which by itself results in the amplitude $A_{m_{\mathcal{P}}}^{\nu}$. The factor $l_{\mathcal{P}}$ is explained in the following way: because of the trace in (4.8), every vertex visited by the prime periodic orbit $m_{\mathcal{P}}$ contributes an amplitude $A_{m_{\mathcal{P}}}^{\nu}$ to the total amplitude $A_m[l]$. Since the prime periodic orbit is of length $l_{\mathcal{P}}$, i.e. it visits $l_{\mathcal{P}}$

vertices, the total contribution is $l_{\mathcal{P}} A_{m_{\mathcal{P}}}^{\nu}$. Finally, if we denote by $L_{m_{\mathcal{P}}}^{(0)}$ the reduced action of the prime periodic orbit $m_{\mathcal{P}}$, then

$$L_m^{(0)}[l] = \nu L_{m_{\mathcal{P}}}^{(0)}. \quad (4.13)$$

Collecting (4.11) – (4.13) and inserting it into (4.10) yields

$$k_n = \bar{k}_n - \frac{2}{\pi} \operatorname{Im} \sum_{m_{\mathcal{P}}} \frac{1}{L_{m_{\mathcal{P}}}^{(0)}} \sum_{\nu=1}^{\infty} \frac{1}{\nu^2} A_{m_{\mathcal{P}}}^{\nu} e^{i\nu L_{m_{\mathcal{P}}}^{(0)} \bar{k}_n} \sin \left[\frac{\nu\pi}{2\omega_0} L_{m_{\mathcal{P}}}^{(0)} \right], \quad (4.14)$$

where the summation is over all prime periodic orbits $m_{\mathcal{P}}$ of the graph and all their repetitions ν . It is important to note here that the summation in (4.14) still has to be performed according to the symbolic lengths $l = \nu l_{\mathcal{P}}$ of the orbits.

In conclusion we note that our methods are generalizable to obtain any differentiable function $f(k_n)$ directly and explicitly. Instead of integrating over $N(k)$ alone in (4.5) we integrate over $f'(k)N(k)$ and obtain

$$f(k_n) = n f(\hat{k}_n) - (n-1) f(\hat{k}_{n-1}) - \int_{\hat{k}_{n-1}}^{\hat{k}_n} f'(k) N(k) dk. \quad (4.15)$$

Following the same logic that led to (4.10), we obtain

$$f(k_n) = n f(\hat{k}_n) - (n-1) f(\hat{k}_{n-1}) - \frac{2}{\pi} \operatorname{Im} \sum_{l=1}^{\infty} \frac{1}{l} \sum_{m \in P[l]} A_m[l] G_n(L_m^{(0)}[l]), \quad (4.16)$$

where

$$G_n(x) = \int_{\hat{k}_{n-1}}^{\hat{k}_n} f'(k) e^{ixk} dk. \quad (4.17)$$

This amounts to a resummation since one can also obtain the series for k_n first, and then form $f(k_n)$.

V. INTERCHANGE OF INTEGRATION AND SUMMATION

One of the key points for the existence of the explicit formula (4.10) is the possibility to interchange integration and summation according to

$$\int_a^b \left(\sum_{n=1}^{\infty} \frac{e^{in\sigma(x)}}{n} \right) dx = \sum_{n=1}^{\infty} \left(\int_a^b \frac{e^{in\sigma(x)}}{n} dx \right), \quad (5.1)$$

where $\sigma(x)$ is continuous and has a continuous first derivative. We will prove (5.1) in two steps.

Step 1: According to a well-known theorem (see, e.g., Ref. [36], volume I, p. 394) summation and integration can be interchanged if the convergence of the sum is uniform. Consider an interval $[\sigma_1, \sigma_2]$ that does not contain a point $\sigma_0 = 0 \pmod{2\pi}$. Define

$$\mathcal{S}(\sigma) = \sum_{n=1}^{\infty} \frac{e^{in\sigma}}{n}. \quad (5.2)$$

Let

$$f(\sigma) = \frac{1}{2} \ln \frac{1}{2[1 - \cos(\sigma)]} + i \frac{\pi - \sigma \pmod{2\pi}}{2}. \quad (5.3)$$

Then, according to formulas F2 and F3 (Appendix B), $\mathcal{S}(\sigma) = f(\sigma)$ in $[\sigma_1, \sigma_2]$. In other words, $\mathcal{S}(\sigma)$ is the Fourier series representation of $f(\sigma)$. According to another well-known theorem (see, e.g., Ref. [37], volume I, pp. 70–71) the Fourier series of a piecewise continuous function converges uniformly in every closed interval in which the function is continuous. Since $f(\sigma)$ is continuous and smooth in $[\sigma_1, \sigma_2]$, $\mathcal{S}(\sigma)$ converges uniformly in $[\sigma_1, \sigma_2]$. This means that summation and integration can be interchanged in any closed interval $[x_1, x_2]$ for which $\sigma(x) \neq 0 \pmod{2\pi} \forall x \in [x_1, x_2]$.

Step 2: Now let there be a single point $x^* \in (x_1, x_2)$ with $\sigma(x^*) = 0 \pmod{2\pi}$. Then, for any $\epsilon_1, \epsilon_2 > 0$ with $x^* - \epsilon_1 \geq x_1$, $x^* + \epsilon_2 \leq x_2$, $\mathcal{S}(\sigma(x))$ is uniformly convergent in $[x_1, x^* - \epsilon_1]$ and $[x^* + \epsilon_2, x_2]$ and integration and summation can be interchanged when integrating over these two intervals. Consequently,

$$\begin{aligned} & \int_{x_1}^{x_2} \left(\sum_{n=1}^{\infty} \frac{e^{in\sigma(x)}}{n} \right) dx = \\ & \int_{x_1}^{x^* - \epsilon_1} \left(\sum_{n=1}^{\infty} \frac{e^{in\sigma(x)}}{n} \right) dx + \int_{x^* - \epsilon_1}^{x^* + \epsilon_2} \left(\sum_{n=1}^{\infty} \frac{e^{in\sigma(x)}}{n} \right) dx + \int_{x^* + \epsilon_2}^{x_2} \left(\sum_{n=1}^{\infty} \frac{e^{in\sigma(x)}}{n} \right) dx = \\ & \sum_{n=1}^{\infty} \left(\int_{x_1}^{x^* - \epsilon_1} \frac{e^{in\sigma(x)}}{n} dx \right) + \sum_{n=1}^{\infty} \left(\int_{x^* + \epsilon_2}^{x_2} \frac{e^{in\sigma(x)}}{n} dx \right) + \int_{x^* - \epsilon_1}^{x^* + \epsilon_2} \left(\sum_{n=1}^{\infty} \frac{e^{in\sigma(x)}}{n} \right) dx. \quad (5.4) \end{aligned}$$

Since $\sum_{n=1}^{\infty} \int_{x_1}^{x^*-\epsilon_1} \exp[in\sigma(x)]/n dx$ and $\sum_{n=1}^{\infty} \int_{x^*+\epsilon_2}^{x_2} \exp[in\sigma(x)]/n dx$ are both uniformly convergent, we have with L11 (Appendix B):

$$\int_{x_1}^{x_2} \left(\sum_{n=1}^{\infty} \frac{e^{in\sigma(x)}}{n} \right) dx = \sum_{n=1}^{\infty} \left[\int_{x_1}^{x^*-\epsilon_1} \frac{e^{in\sigma(x)}}{n} dx + \int_{x^*+\epsilon_2}^{x_2} \frac{e^{in\sigma(x)}}{n} dx \right] + \int_{x^*-\epsilon_1}^{x^*+\epsilon_2} \left(\sum_{n=1}^{\infty} \frac{e^{in\sigma(x)}}{n} \right) dx. \quad (5.5)$$

Since $\exp[in\sigma(x)]/n$ is a non-singular, smooth function at $x = x^*$, there is no problem with taking $\epsilon_1, \epsilon_2 \rightarrow 0$ for the first two integrals on the right-hand side of (5.5). Therefore, integration and summation on the left-hand side of (5.5) can be interchanged if

$$\lim_{\epsilon_1, \epsilon_2 \rightarrow 0} \int_{x^*-\epsilon_1}^{x^*+\epsilon_2} \left(\sum_{n=1}^{\infty} \frac{e^{in\sigma(x)}}{n} \right) dx = 0 = \lim_{\epsilon_1, \epsilon_2 \rightarrow 0} \sum_{n=1}^{\infty} \left(\int_{x^*-\epsilon_1}^{x^*+\epsilon_2} \frac{e^{in\sigma(x)}}{n} dx \right). \quad (5.6)$$

This is guaranteed according to T3 (Appendix A). Assuming that $\sigma(x)$ has only a finite number N of zeros mod 2π in (a, b) , we can break (a, b) into N sub-intervals containing a single zero only, in which the interchange of summation and integration is allowed. This proves (5.1).

Returning to the crucial step from (4.7) to (4.8) we have to show that

$$\int_{k_1}^{k_2} \sum_{n=1}^{\infty} \frac{1}{n} S^n(k) dk = \sum_{n=1}^{\infty} \frac{1}{n} \int_{k_1}^{k_2} S^n(k) dk. \quad (5.7)$$

Since $S(k)$ is unitary, it is diagonalizable, i.e. there exists a matrix $W(k)$ such that

$$S(k) = W(k) \text{diag} \left(e^{i\sigma_1(k)}, \dots, e^{i\sigma_{2N_B}(k)} \right) W^\dagger(k), \quad (5.8)$$

where $\sigma_1(k), \dots, \sigma_{2N_B}(k)$ are the $2N_B$ eigenphases of $S(k)$. Because of the structure (2.2) of the S matrix in conjunction with the smoothly varying phases (2.3), the eigenphases of the S matrix have only a finite number of zeros mod 2π in any finite interval of k . This is important for later use of (5.1) which was only proved for this case.

We now make essential use of our focus on finite quantum graphs, which entails a finite-dimensional S matrix, and therefore a finite-dimensional matrix W . In this case matrix multiplication with W leads only to finite sums. Since for finite sums integration and

summation is always interchangeable we have

$$\int_{k_1}^{k_2} \sum_{n=1}^{\infty} \frac{1}{n} S^n(k) dk = \int_{k_1}^{k_2} W(k) \sum_{n=1}^{\infty} \text{diag} \left(\frac{e^{in\sigma_1(k)}}{n}, \dots, \frac{e^{in\sigma_{2N_B}(k)}}{n} \right) W^\dagger(k) dk \stackrel{(5.1)}{=} \sum_{n=1}^{\infty} \int_{k_1}^{k_2} W(k) \text{diag} \left(\frac{e^{in\sigma_1(k)}}{n}, \dots, \frac{e^{in\sigma_{2N_B}(k)}}{n} \right) W^\dagger(k) dk = \sum_{n=1}^{\infty} \frac{1}{n} \int_{k_1}^{k_2} S^n(k) dk. \quad (5.9)$$

This equation justifies the step from (4.7) to (4.8), which proves the validity of (4.10) and (4.14).

VI. CONVERGENCE PROPERTIES OF THE PERIODIC ORBIT SERIES

In this section we prove rigorously that (4.14) contains conditionally convergent as well as absolutely convergent cases. We accomplish this by investigating the convergence properties of (4.14) in the case of the dressed three-vertex linear graph shown in Fig. 5. The potential on the bond B_{12} is zero; the potential on the bond B_{23} is a scaling potential explicitly given by

$$U_{23} = \lambda E, \quad (6.1)$$

where E is the energy of the quantum particle and λ is a real constant with $0 < \lambda < 1$. The quantum graph shown in Fig. 5 was studied in detail in [8–12,29]. Denoting by a the geometric length of the bond B_{12} and by b the geometric length of the bond B_{23} , its spectral equation is given by [8–12,29]

$$\sin(\omega_0 k) = r \sin(\omega_1 k), \quad (6.2)$$

where

$$\omega_0 = a + \beta b, \quad \omega_1 = a - \beta b, \quad r = \frac{1 - \beta}{1 + \beta}, \quad \beta = \sqrt{1 - \lambda}. \quad (6.3)$$

With

$$\gamma_0 = 1/2, \quad a_1 = r, \quad \gamma_1 = 1/2, \quad (6.4)$$

the spectral equation (6.2) is precisely of the form (2.14). Since according to (6.3) $a_1 = r < 1$, the regularity condition (3.1) is fulfilled and (6.2) is the spectral equation of a regular quantum graph. This means that we can apply (4.14) for the computation of the solutions of (6.2). In order to do so, we need a scheme for enumerating the periodic orbits of the three-vertex linear graph. It was shown in [29] that a one-to-one correspondence exists between the periodic orbits of the three-vertex linear graph and the set of binary Pólya necklaces [29,38,39]. A binary necklace is a string of two symbols arranged in a circle such that two necklaces are different if (a) they are of different lengths or (b) they are of the same length but cannot be made to coincide even after applying cyclic shifts of the symbols of one of the necklaces. For the graph of Fig. 5 it is convenient to introduce the two symbols \mathcal{L} and \mathcal{R} , which can be interpreted physically as the reflection of a graph particle from the left (V_1) or the right (V_3) dead-end vertices, respectively. Since strings of symbols are frequently referred to as words, we adopt the symbol w to denote a particular necklace. For a given necklace w it is convenient to define the following functions [29]: $n_{\mathcal{R}}(w)$, which counts the number of \mathcal{R} s in w , $n_{\mathcal{L}}(w)$, which counts the number of \mathcal{L} s in w , the pair function $\alpha(w)$, which counts all occurrences of \mathcal{R} -pairs or \mathcal{L} -pairs in w and the function $\beta(w)$, which counts all occurrences of \mathcal{LR} or \mathcal{RL} symbol combinations in w . We also define the function $\ell(w) = n_{\mathcal{L}}(w) + n_{\mathcal{R}}(w)$, which returns the total binary length of the word w , and the phase function $\chi(w)$, defined as the sum of $\ell(w)$ and the number of \mathcal{R} -pairs in w . We note the identity

$$\alpha(w) + \beta(w) = \ell(w). \quad (6.5)$$

In evaluating the functions defined above, we have to be very careful to take note of the cyclic nature of binary necklaces. Therefore, for example, $\alpha(\mathcal{R}) = 1$, $\beta(\mathcal{LR}) = 2$, $\alpha(\mathcal{LLRRRL}) = 3$ and $\beta(\mathcal{LLRRRL}) = 2$, which also checks (6.5). In addition we define the set $W(l)$ of all binary necklaces of length l .

Let us look at $W(2)$. This set contains three necklaces, \mathcal{LL} , $\mathcal{LR} = \mathcal{RL}$ (cyclic rotation of symbols) and \mathcal{RR} . The necklace \mathcal{LL} is not a primitive necklace, since it consists of a repetition of the primitive symbol \mathcal{L} . The same holds for the necklace \mathcal{RR} , which is a

repetition of the primitive symbol \mathcal{R} . The necklace \mathcal{LR} is primitive, since it cannot be written as a repetition of a shorter string of symbols. This motivates the definition of the set $W_{\mathcal{P}}$ of all primitive binary necklaces and the set $W_{\mathcal{P}}(l)$ containing all primitive binary necklaces of length l .

An important question arises: How many primitive necklaces $N_{\mathcal{P}}(l)$ are there in $W(l)$? In other words, how many members are there in $W_{\mathcal{P}}(l) \subset W(l)$? The following formula gives the answer [39]:

$$N_{\mathcal{P}}(l) = \frac{1}{l} \sum_{m|l} \phi(m) 2^{l/m}, \quad (6.6)$$

where the symbol “ $m|l$ ” denotes “ m is a divisor of l ”, and $\phi(m)$ is Euler’s totient function defined as the number of positive integers smaller than m and relatively prime to m with $\phi(1) = 1$ as a useful convention. It is given explicitly by [40]

$$\phi(1) = 1, \quad \phi(n) = n \prod_{p|n} \left(1 - \frac{1}{p}\right), \quad n \geq 2, \quad (6.7)$$

where p is a prime number. Thus the first four totients are given by $\phi(1) = 1$, $\phi(2) = 1$, $\phi(3) = 2$ and $\phi(4) = 2$.

A special case of (6.6) is the case in which l is a prime number. In this case we have explicitly

$$N_{\mathcal{P}}(p) = \frac{1}{p} (2^p - 2), \quad p \text{ prime.} \quad (6.8)$$

This is immediately obvious from the following combinatorial argument. By virtue of p being a prime number a necklace of length p cannot contain an integer repetition of shorter substrings, except for strings of length 1 or length p . Length p is trivial. It corresponds to the word itself. Length 1 leads to the two cases $\mathcal{RRRRR}\dots\mathcal{R}$ and $\mathcal{LLLLL}\dots\mathcal{L}$, where the symbols \mathcal{R} and \mathcal{L} , respectively, are repeated p times. So, except for these two special necklaces, any necklace of prime length p is automatically primitive. Thus there are

$$\frac{1}{p} \binom{p}{\nu} \quad (6.9)$$

different necklaces with ν symbols \mathcal{L} and $p - \nu$ symbols \mathcal{R} , where the factor $1/p$ takes care of avoiding double counting of cyclically equivalent necklaces. In total, therefore, we have

$$N_{\mathcal{P}}(p) = \frac{1}{p} \sum_{\nu=1}^{p-1} \binom{p}{\nu} = \frac{1}{p} (2^p - 2) \quad (6.10)$$

primitive necklaces of length p , in agreement with (6.8). The sum in (6.10) ranges from 1 to $p - 1$ since $\nu = 0$ would correspond to the composite, non-primitive necklace $\mathcal{R}\mathcal{R}\mathcal{R}\mathcal{R}\dots\mathcal{R}$ and $\nu = p$ would correspond to the composite, non-primitive necklace $\mathcal{L}\mathcal{L}\mathcal{L}\mathcal{L}\dots\mathcal{L}$.

We are now ready to apply (4.14) to the three-vertex linear graph. In “necklace notation” it is given by [8–12,29]

$$k_n = \bar{k}_n - \frac{2}{\pi} \sum_{l=1}^{\infty} \sum_{\nu=1}^{\infty} \sum_{w \in W_{\mathcal{P}}: \nu w \in W(l)} \frac{A_w^{\nu}}{\nu^2 L_w^{(0)}} \sin \left[\nu L_w^{(0)} \bar{k}_n \right] \sin \left[\frac{\nu \pi}{2\omega_0} L_w^{(0)} \right], \quad (6.11)$$

where $L_w^{(0)}$ is the reduced action of the primitive necklace w , given by [29]

$$L_w^{(0)} = 2[n_{\mathcal{L}}(w)a + n_{\mathcal{R}}(w)\beta b] \quad (6.12)$$

and the amplitude A_w of the primitive necklace w is given by [29]

$$A_w = (-1)^{\chi(w)} r^{\alpha(w)} (1 - r^2)^{\beta(w)/2}, \quad (6.13)$$

where r and β are defined in (6.3). The notation νw refers to a necklace of binary length $\nu \ell(w)$ that consists of ν concatenated substrings w . Note that the summations in (6.11) are ordered in such a way that for fixed l we sum over all possible primitive words w and their repetitions ν such that the total length of the resulting binary necklace amounts to l , and only then do we sum over the binary length l of the necklaces. This summation scheme, explicitly specified in (6.11), complies completely with the summation scheme defined in Sec. IV. Since we proved in Sec. IV that (4.14) converges, provided we adhere to the correct summation scheme, so does (6.11).

A numerical example of the computation of the spectrum of (6.2) via (6.11) was presented in [8] where we chose $a = 0.3$, $b = 0.7$ and $\lambda = 1/2$. For $n = 1, 10, 100$ we computed the exact roots of (6.2) numerically by using a simple numerical root-finding algorithm. We obtained

$k_1^{(\text{exact})} \approx 4.107149$, $k_{10}^{(\text{exact})} \approx 39.305209$ and $k_{100}^{(\text{exact})} \approx 394.964713$. Next we computed these roots using the explicit formula (6.11). Including all binary necklaces up to $l = 20$, which amounts to including a total of approximately 10^5 primitive periodic necklaces, we obtained $k_1^{(\text{p.o.})} \approx 4.105130$, $k_{10}^{(\text{p.o.})} \approx 39.305212$ and $k_{100}^{(\text{p.o.})} \approx 394.964555$. Given the fact that in Sec. IV we proved exactness and convergence of (4.14) ((6.11), respectively), the good agreement between $k_n^{(\text{exact})}$ and $k_n^{(\text{p.o.})}$, $n = 1, 10, 100$, is not surprising. Nevertheless we found it important to present this simple example here, since it illustrates the abstract procedures and results obtained in Sec. IV, checks our algebra and instills confidence in our methods.

We now investigate the convergence properties of (6.11) for two special cases of dressed linear three-vertex quantum graphs (see Fig. 5) defined by

$$r = \frac{1}{\sqrt{2}}, \quad a = m\beta b, \quad m = 1, 2. \quad (6.14)$$

In this case the reduced actions (6.12) reduce to

$$L_w^{(0)} = 2a[n_{\mathcal{L}}(w) + n_{\mathcal{R}}(w)/m] \quad (6.15)$$

and ω_0 is given by

$$\omega_0 = a \left(1 + \frac{1}{m} \right). \quad (6.16)$$

Using (6.5), the amplitudes (6.13) are

$$A_w = (-1)^{\chi(w)} 2^{-\ell(w)/2}. \quad (6.17)$$

We now show that for $m = 1$ the first sin-term in (6.11) is always zero, and thus (6.11) converges (trivially) absolutely in this case. For $m = 1$ (6.15) becomes

$$L_w^{(0)} = 2a[n_{\mathcal{L}}(w) + n_{\mathcal{R}}(w)] = 2a\ell(w). \quad (6.18)$$

Also, according to (3.3) and (6.4) \bar{k}_n is given by

$$\bar{k}_n = \frac{\pi}{\omega_0} [n + \mu + 1]. \quad (6.19)$$

Thus, for $m = 1$ the argument of the first sin-term in (6.11) is given by

$$\nu L_w^{(0)} \bar{k}_n = \nu \ell(w)(n + \mu + 1)\pi. \quad (6.20)$$

This is an integer multiple of π , and thus all terms in the periodic-orbit sum of (6.11) vanish identically. Therefore we proved that there exists at least one case in which the periodic-orbit sum in (6.11) is (trivially) absolutely convergent.

We now prove rigorously that there exists at least one non-trivial case in which (6.11) converges only conditionally. Since we already proved in Sec. IV that (6.11) always converges, all we have to prove is that there exists a case in which the sum of the absolute values of the terms in (6.11) diverges. In order to accomplish this, let us focus on the case $m = 2$ and estimate the sum

$$s = \sum_{l=1}^{\infty} \sum_{\nu=1}^{\infty} \sum_{w \in W_{\mathcal{P}}: \nu w \in W(l)} \left| \frac{1}{\nu^2 L_w^{(0)} 2^{\ell(w)/2}} \sin \left[\nu L_w^{(0)} \bar{k}_n \right] \sin \left[\frac{\nu \pi}{2\omega_0} L_w^{(0)} \right] \right|. \quad (6.21)$$

We now restrict the summation over all integers l to the summation over prime numbers p only. Moreover, we discard all non-primitive necklaces of length p , which is equivalent to keeping terms with $\nu = 1$ only. Observing that trivially $\ell(w) = p$ for all necklaces in $W_{\mathcal{P}}(p)$, we obtain:

$$s \geq \sum_p \sum_{w \in W_{\mathcal{P}}(p)} \left| \frac{1}{L_w^{(0)} 2^{p/2}} \sin \left[L_w^{(0)} \bar{k}_n \right] \sin \left[\frac{\pi}{2\omega_0} L_w^{(0)} \right] \right|, \quad (6.22)$$

where the sum is over all prime numbers p . For $m = 2$ the reduced actions are given by

$$L_w^{(0)} = a[2n_{\mathcal{L}}(w) + n_{\mathcal{R}}(w)] \quad (6.23)$$

and

$$\omega_0 = \frac{3a}{2}, \quad \bar{k}_n = \frac{2\pi}{3a}(n + \mu + 1). \quad (6.24)$$

We use these relations to evaluate the arguments of the two sin-functions in (6.22). We obtain

$$L_w^{(0)} \bar{k}_n = \frac{2\pi}{3}[2n_{\mathcal{L}}(w) + n_{\mathcal{R}}(w)](n + \mu + 1) \quad (6.25)$$

and

$$\frac{\pi}{2\omega_0} L_w^{(0)} = \frac{\pi}{3} [2n_{\mathcal{L}}(w) + n_{\mathcal{R}}(w)], \quad (6.26)$$

respectively. We see immediately that all terms in (6.22) are zero if $n + \mu + 1$ is divisible by 3. This provides additional examples of (trivially) absolutely convergent cases of (6.11). In case $n + \mu + 1$ is not divisible by 3, only those terms contribute to (6.22) for which $2n_{\mathcal{L}}(w) + n_{\mathcal{R}}(w)$ is not divisible by 3. Following the reasoning that led to (6.10), $n_{\mathcal{L}}(w)$ ranges from 1 to $p - 1$ for $w \in W_{\mathcal{P}}(p)$. Then, $2n_{\mathcal{L}}(w) + n_{\mathcal{R}}(w)$ ranges from $p + 1$ to $2p - 1$ in steps of 1. Since $p + 3j$ is never divisible by 3 for p prime and $j \in \mathbf{N}$, the number of primitive necklaces w of length p with the property that $2n_{\mathcal{L}}(w) + n_{\mathcal{R}}(w)$ is not divisible by 3 is at least

$$\frac{1}{p} \left\{ \binom{p}{3} + \binom{p}{6} + \dots \right\} = \frac{1}{3p} \left[2^p + 2 \cos\left(\frac{p\pi}{3}\right) - 3 \right], \quad (6.27)$$

where the sum over the binomial coefficients was evaluated with the help of formula 0.1521 in [41]. Therefore, with (6.23), (6.25), (6.26), (6.27), $|\sin(2j\pi/3)| = \sqrt{3}/2$ for all $j \in \mathbf{N}$ and $2n_{\mathcal{L}}(w) + n_{\mathcal{R}}(w) \leq 2p - 1$ for $w \in W_{\mathcal{P}}(p)$, we obtain

$$s \geq \frac{1}{4a} \sum_p \frac{1}{p(2p-1)2^{p/2}} \left[2^p + 2 \cos\left(\frac{p\pi}{3}\right) - 3 \right], \quad (6.28)$$

which obviously diverges exponentially. The physical reason is that the quantum amplitudes, which contribute the factor $2^{-p/2}$ in (6.28) are not able to counteract the proliferation 2^p of primitive periodic orbits (primitive binary necklaces) in (6.28). Analogous results can easily be obtained for graphs with $m > 2$ in (6.14).

In summary we established in this section that the convergence properties of (4.14) depend on the details of the quantum graph under investigation. We proved rigorously that both conditionally convergent and absolutely convergent cases can be found. We emphasize that the degree of convergence does not change the fact, proved in Sec. IV, that (4.14) always converges, and always converges to the exact spectral eigenvalues.

VII. LAGRANGE'S INVERSION FORMULA

The periodic orbit expansions presented in Sec. IV are not the only way to obtain the spectrum of regular quantum graphs explicitly. Lagrange's inversion formula [42] offers an alternative route. Given an implicit equation of the form

$$x = a + w\varphi(x), \quad (7.1)$$

Lagrange's inversion formula determines a root x^* of (7.1) according to the explicit series expansion

$$x^* = a + \sum_{\nu=1}^{\infty} \frac{w^\nu}{\nu!} \frac{d^{\nu-1}}{dx^{\nu-1}} \varphi^\nu(x) \Big|_a, \quad (7.2)$$

provided $\varphi(x)$ is analytic in an open interval I containing x^* and

$$|w| < \left| \frac{x-a}{\varphi(x)} \right| \quad \forall x \in I. \quad (7.3)$$

Since (3.2) is of the form (7.1), and the regularity condition (3.1) ensures that (7.3) is satisfied, we can use Lagrange's inversion formula (7.2) to compute explicit solutions of (2.14).

In order to illustrate Lagrange's inversion formula we will now apply it to the solution of (6.2). Defining $x = \omega_0 k$, the n th root of (6.2) satisfies the implicit equation

$$x_n = \pi n + (-1)^n \arcsin[r \sin(\rho x_n)], \quad (7.4)$$

where $\rho = \omega_1/\omega_0$ and $|\rho| < 1$. For the same parameter values as specified in [8] and already used above in Sec. VI we obtain $x_1^{(\text{exact})} = \omega_0 k_1^{(\text{exact})} \approx 3.265080$, $x_{10}^{(\text{exact})} = \omega_0 k_{10}^{(\text{exact})} \approx 31.246649$ and $x_{100}^{(\text{exact})} = \omega_0 k_{100}^{(\text{exact})} \approx 313.986973$. We now re-compute these values using the first two terms in the expansion (7.2). For our example they are given by

$$x_n^{(2)} = \pi n + \arcsin[r \sin(\rho \pi n)] \left\{ (-1)^n + \frac{r \rho \cos(\rho \pi n)}{\sqrt{1 - r^2 \sin^2(\rho \pi n)}} \right\}. \quad (7.5)$$

We obtain $x_1^{(2)} = 3.265021 \dots$, $x_{10}^{(2)} = 31.246508 \dots$ and $x_{100}^{(2)} = 313.986819 \dots$, in very good agreement with $x_1^{(\text{exact})}$, $x_{10}^{(\text{exact})}$ and $x_{100}^{(\text{exact})}$.

Although both, (4.14) and (7.2) are exact, and, judging from our example, (7.2) appears to converge very quickly, the main difference between (4.14) and (7.2) is that no physical insight can be obtained from (7.2), whereas (4.14) is tightly connected to the classical mechanics of the graph system providing, in the spirit of Feynman’s path integrals, an intuitively clear picture of the physical processes in terms of a superposition of amplitudes associated with classical periodic orbits.

VIII. DISCUSSION, SUMMARY AND CONCLUSION

There are only very few exact results in quantum chaos theory. In particular not much is known about the convergence properties of periodic orbit expansions. Since quantum graphs are an important model for quantum chaos [43], which in fact have already been called “paradigms of quantum chaos” [25], it seems natural that they provide a logical starting point for the mathematical investigation of quantum chaos. The regular quantum graphs defined in this paper are important because they provide the first example of an explicitly solvable quantum chaotic system. Moreover regular quantum graphs allow us to prove two important results: (a) Not all periodic orbit expansions diverge. There exist nontrivial, convergent, periodic orbit expansions. (b) There exist explicit periodic orbit expansions that converge to the exact values of individual spectral points.

The main result of this paper is an analytical proof of the validity and the convergence of the explicit spectral formulas (4.10) and (4.14), respectively. This result is novel in two respects. (i) While periodic orbit expansions of the spectral density and the spectral staircase of a quantum system are basic tools of quantum chaos, the very concept of a periodic orbit expansion for individual spectral eigenvalues is new. (ii) Due to the exponential proliferation of the number of periodic orbits with their (action) lengths, it is frequently assumed in the quantum chaos community that periodic orbit expansions are formal tools at best, but do not converge. We proved in this paper that, at least as far as regular quantum graphs are concerned, and despite the exponential proliferation of periodic orbits in this case [8], the

periodic orbit expansion (4.14) converges in the usual sense of elementary analysis. This result is also new.

The main ingredient in the proof of (4.14) is theorem T2 (Appendix A), i.e. an analytical proof that there is exactly one spectral point in every root cell I_n . In discussions with our colleagues we found that while many pointed out the necessity of justifying the interchange of integration and summation in (5.1) (now established in Sec. V with T3 (Appendix A)), many were initially puzzled by the existence of root intervals and the organization of the spectral points into root cells, now guaranteed by T2 (Appendix A). This is so because regular quantum graphs have a positive topological entropy [2,6,8] and are in this sense quantum chaotic systems. Hence the spectrum of regular quantum graphs is expected to be “wild”, in complete contrast to the fact, proved in this paper, that the spectrum of regular quantum graphs can actually be organized into regular root cells. In this sense regular quantum graphs are closely related to other quantum chaotic systems that also show marked deviations from the expected universal behavior [6,7,44]. As a specific example we mention chaotic billiards on the hyperbolic plane generated by arithmetic groups [45]. We hope that the pedagogical presentation of the proofs in Appendices A and B, with their hierarchical structure and the use of only elementary analysis concepts will help to establish theorems T2 and T3 (Appendix A), and their consequence, the existence of explicit, convergent periodic orbit expansions. We mention that the spectral equation (2.14) of a finite quantum graph is an example of an almost periodic function [46]. More information on the analytical structure of the zeros of almost periodic functions can be found in [47].

There are many basic quantum mechanical problems that lead to transcendental equations of the type (2.14). So far the recommended method is to solve them graphically or numerically (see, e.g., [48,49]). Based on the results presented in this paper, a third method is now available for presentation in text books on quantum mechanics: explicit analytical solutions. When the regularity condition (3.1) is satisfied, either the Lagrangian inversion method or the periodic orbit expansion (4.14) may be employed. Since the Lagrangian method is a purely mathematical tool without immediate physical meaning, the periodic

orbit expansion may be preferred due to its direct physical relevance in terms of concrete classical physics.

Having been established with mathematical rigor in this paper, formula (4.14) may serve as the starting point for many further investigations. We mention one: Since according to (4.14) k_n is known explicitly, so is the level spacing $s_n = k_n - k_{n-1}$. This may give us an important handle on investigating analytically and exactly the nearest-neighbor spacing statistics $P(s)$ [6,44] of regular quantum graphs. Whatever the precise properties of $P(s)$ will be, one result is clear already: due to the existence of the root-free zones F_n , established in Sec. III, $P(s)$ is not Wignerian. Thus, regular quantum graphs will join the growing class of classically chaotic systems which do not show the generic properties of typical quantum chaotic systems.

A corollary of some significance is the following. Since we proved that for regular quantum graphs there is exactly one root k_n of (2.14) in I_n , this proves rigorously that for regular quantum graphs the number of roots of (2.14) smaller than k grows like $\bar{N}(k) \sim \omega_0 k / \pi$ (Weyl's law [6]).

An open question is the generalization of our results to the case of infinite quantum graphs. In case $\sum_{i=1}^{\infty} |a_i|$ converges, it seems straightforward to generalize the regularity condition (3.1) to the case of infinite quantum graphs.

In summary we proved a rigorous theorem on the existence and convergence of explicit periodic orbit expansions of the spectral points of regular quantum graphs. We hope that this paper will lay the foundation for further rigorous research in quantum graph theory.

IX. ACKNOWLEDGMENTS

Y.D. and R.B. gratefully acknowledge financial support by NSF grant PHY-9900730 and PHY-9984075; Y.D. by NSF grant PHY-9900746.

X. APPENDIX A: THEOREMS

Theorem T1: Let $a_i, \omega_i, \alpha_i \in \mathbf{R}$, $i \in I := \{1, \dots, N\}$, $N \in \mathbf{N}$, $\sum_{i=1}^N |a_i| < 1$, and $|\omega_i| < 1$.

Then:

$$f(x) := \frac{\left[\sum_{i=1}^N a_i \omega_i \sin(\omega_i x + \alpha_i) \right]^2}{1 - \left[\sum_{i=1}^N a_i \cos(\omega_i x + \alpha_i) \right]^2} < 1 \quad \forall x \in \mathbf{R}. \quad (10.1)$$

Proof: Define $\theta_i := \omega_i x + \alpha_i$, $i \in I$. Then:

$$f(x) \leq \frac{\left[\sum_{i=1}^N |a_i| |\omega_i| |\sin(\theta_i)| \right]^2}{1 - \left[\sum_{i=1}^N |a_i| |\cos(\theta_i)| \right]^2} < \frac{\left[\sum_{i=1}^N |a_i| |\sin(\theta_i)| \right]^2}{1 - \left[\sum_{i=1}^N |a_i| |\cos(\theta_i)| \right]^2}. \quad (10.2)$$

Define the three functions:

$$S(\vec{x}) := \sum_{i=1}^N |a_i| \sin(x_i), \quad C(\vec{x}) := \sum_{i=1}^N |a_i| \cos(x_i), \quad g(\vec{x}) := \frac{S^2(\vec{x})}{1 - C^2(\vec{x})}, \quad (10.3)$$

where $\vec{x} := (x_1, \dots, x_N) \in \mathbf{R}^N$. Since there is always an \vec{x} such that $|\sin(\theta_i)| = \sin(x_i)$, $|\cos(\theta_i)| = \cos(x_i)$, we prove T1 by showing that $g(\vec{x}) \leq 1 \quad \forall \vec{x} \in \mathbf{R}^N$. Because of $C^2(\vec{x}) = \sum_{ij} |a_i| |a_j| \cos(x_i) \cos(x_j) \leq \sum_{ij} |a_i| |a_j| = (\sum_i |a_i|)^2 < 1 \quad \forall \vec{x} \in \mathbf{R}^N$, the function g is well-defined and singularity-free in \mathbf{R}^N . Since g is differentiable in \mathbf{R}^N we prove $g \leq 1$ by looking for the extrema of g :

$$\frac{\partial g(\vec{x})}{\partial x_k} = 0 \quad \Rightarrow \quad (1 - C^2(\vec{x}))S(\vec{x}) \cos(x_k) - S^2(\vec{x})C(\vec{x}) \sin(x_k) = 0, \quad k \in I. \quad (10.4)$$

Let \vec{x}^* be a solution of (10.4). There are three different cases. (i) $S(\vec{x}^*) = 0$. In this case we have $g(\vec{x}^*) = 0 < 1$. (ii) $C(\vec{x}^*) = 0$ and $S(\vec{x}^*) \neq 0$. In this case we have $g(\vec{x}^*) = S^2(\vec{x}^*) < 1$. (iii) $C(\vec{x}^*) \neq 0$ and $S(\vec{x}^*) \neq 0$. In this case (10.4) reduces to

$$\sin(x_k^*) = \frac{(1 - C^2(\vec{x}^*))}{S(\vec{x}^*)C(\vec{x}^*)} \cos(x_k^*), \quad k \in I. \quad (10.5)$$

For g evaluated at \vec{x}^* of (10.5) we obtain:

$$g(\vec{x}^*) = \left[\frac{1 - C^2(\vec{x}^*)}{S(\vec{x}^*)C(\vec{x}^*)} \right]^2 \frac{\left[\sum_{i=1}^N |a_i| \cos(x_i^*) \right]^2}{1 - C^2(\vec{x}^*)} = \frac{1 - C^2(\vec{x}^*)}{S^2(\vec{x}^*)} = \frac{1}{g(\vec{x}^*)}. \quad (10.6)$$

This implies $g^2(\bar{x}^*) = 1$, or, since $g \geq 0$ in \mathbf{R}^N , $g(\bar{x}^*) = 1$. Since there are no boundaries to consider where absolute maxima of g might be located, the local extrema of g encompass all the maxima of g in \mathbf{R}^N and we have $g \leq 1$ in \mathbf{R}^N . This proves T1.

Theorem T2: Consider the spectral equation

$$F(x) := \cos(x) - \Phi(x) = 0, \quad (10.7)$$

where

$$\Phi(x) = \sum_{i=1}^N a_i \cos(\omega_i x + \alpha_i) \quad (10.8)$$

with $a_i, \omega_i, \alpha_i, x \in \mathbf{R}$, $i \in I := \{1, \dots, N\}$, $N \in \mathbf{N}$, $\sum_{i=1}^N |a_i| < 1$, and $|\omega_i| < 1$. Then there is exactly one zero x_n^* of (10.7) in every open interval $I_n = (\nu_n, \nu_{n+1})$, $\nu_n = n\pi$, $n \in \mathbf{Z}$.

Proof:

(i) First we observe that $|\Phi(x)| \leq \sum_{i=1}^N |a_i| < 1 \forall x \in \mathbf{R}$.

(ii) We use (i) to verify that the points ν_n are not roots of (10.7): $|F(\nu_n)| = |(-1)^n - \Phi(\nu_n)| \geq 1 - |\Phi(\nu_n)| \stackrel{(i)}{>} 0$. This means that roots of (10.7) are indeed found only in the *open* intervals I_n .

(iii) We define the closures $\bar{I}_n = [\nu_n, \nu_{n+1}]$. In \bar{I}_n we define ξ according to

$$x = \nu_n + \xi, \quad 0 \leq \xi \leq \pi. \quad (10.9)$$

Inserting (10.9) into (10.7) we see that in \bar{I}_n the spectral function $F(x)$ is identical with

$$f_n(\xi) = (-1)^n \cos(\xi) - \varphi_n(\xi), \quad (10.10)$$

where

$$\varphi_n(\xi) = \sum_{i=1}^N a_i \cos(\omega_i \xi + \alpha_i + n\pi\omega_i). \quad (10.11)$$

(iv) Because of (i): $\text{sign } F(\nu_n) = (-1)^n$. We use this fact to show: $\text{sign } F(\nu_n)F(\nu_{n+1}) = (-1)^{2n+1} = -1$. Since F is continuous, this proves that there is at least one root of F in every I_n , $n \in \mathbf{Z}$.

(v) According to (iii) and (10.10) the roots of F in I_n satisfy $(-1)^n \cos(\xi) = \varphi_n(\xi)$, or

$$\xi = \beta_n(\xi), \quad (10.12)$$

where $\beta_n(\xi) = \arccos[(-1)^n \varphi_n(\xi)]$. Therefore, roots of F are fixed points of β_n .

(vi) In \bar{I}_n :

$$[\beta'_n(\xi)]^2 = \frac{\left[\sum_{i=1}^N a_i \omega_i \sin(\omega_i \xi + \alpha_i + n\pi \omega_i) \right]^2}{1 - \left[\sum_{i=1}^N a_i \cos(\omega_i \xi + \alpha_i + n\pi \omega_i) \right]^2} \stackrel{T1}{<} 1 \Rightarrow \beta'_n(\xi) < 1. \quad (10.13)$$

(vii) Because of (vi) the conditions for L16 are fulfilled and β_n has at most one fixed point in I_n . This means that F has at most one root in I_n . Since according to (iv) there is at least one root of F in I_n , it follows that F has exactly one root in I_n .

Theorem T3:

$$\lim_{\epsilon_1, \epsilon_2 \rightarrow 0} \int_{x^* - \epsilon_1}^{x^* + \epsilon_2} \left(\sum_{n=1}^{\infty} \frac{e^{in\sigma(x)}}{n} \right) dx = 0 = \lim_{\epsilon_1, \epsilon_2 \rightarrow 0} \sum_{n=1}^{\infty} \left(\int_{x^* - \epsilon_1}^{x^* + \epsilon_2} \frac{e^{in\sigma(x)}}{n} dx \right), \quad (10.14)$$

where $\epsilon_1, \epsilon_2 > 0$, $\sigma(x^*) \bmod 2\pi = 0$ and $\sigma(x)$ is continuous and has a continuous first derivative.

Proof:

The two limits in (10.14) are independent. Therefore, splitting the integration range into two pieces (allowed with L11), one from $x^* - \epsilon_1$ to x^* , and the other from x^* to $x^* + \epsilon_2$, it is enough to prove

$$\lim_{\epsilon \rightarrow 0} \int_{x^*}^{x^* + \epsilon} \left(\sum_{n=1}^{\infty} \frac{e^{in\sigma(x)}}{n} \right) dx = 0 = \lim_{\epsilon \rightarrow 0} \sum_{n=1}^{\infty} \left(\int_{x^*}^{x^* + \epsilon} \frac{e^{in\sigma(x)}}{n} dx \right), \quad (10.15)$$

where $\epsilon > 0$. The case $\epsilon < 0$, covering the other integral in (10.14) is treated in complete analogy. The first equality in (10.15) follows immediately from F2, F3 and the fact that according to L20 the real part has a Riemann-integrable log singularity at $x = x^*$ and the imaginary part has a Riemann-integrable jump-singularity at $x = x^*$. The second equality is more difficult to prove.

For the following considerations we assume $\sigma'(x^*) \neq 0$. We will comment on the case $\sigma'(x^*) = 0$ below. According to L10 $\exists \epsilon^* > 0 : f(x) = \sigma'(x)/\sigma'(x^*) > 1/2$, for $|x - x^*| < \epsilon^*$.

Let $\epsilon < \epsilon^*$:

$$\left| \int_{x^*}^{x^*+\epsilon} \frac{\exp[in\sigma(x)]}{n} dx \right| \stackrel{\text{L10}}{<} \left| \int_{x^*}^{x^*+\epsilon} \frac{\exp[in\sigma(x)]}{n} 2 \frac{\sigma'(x)}{\sigma'(x^*)} dx \right| = \frac{2}{n^2 |\sigma'(x^*)|} |\exp[in\sigma(x^* + \epsilon)] - 1| \leq \frac{4}{n^2 |\sigma'(x^*)|}, \quad (10.16)$$

where the last estimate is a simple consequence of the fact that the exponential function is unimodular. While this simple estimate will be useful later on for the case of large n , we need a better estimate for small n :

$$|\exp[in\sigma(x^* + \epsilon)] - 1| = \left| \exp \left\{ in\epsilon \frac{[\sigma(x^* + \epsilon) - \sigma(x^*)]}{\epsilon} \right\} - 1 \right|. \quad (10.17)$$

Now because $\sigma(x)$ is differentiable, we have according to the intermediate value theorem of differential calculus: $\exists \xi(\epsilon) : [\sigma(x^* + \epsilon) - \sigma(x^*)]/\epsilon = \sigma'(\xi)$; $\xi \in [x^*, x^* + \epsilon]$. Therefore:

$$|\exp[in\sigma(x^* + \epsilon)] - 1| = |\exp[in\sigma'(\xi)\epsilon] - 1| \stackrel{\text{L6}}{<} 2|n\sigma'(\xi)\epsilon| = 2n\epsilon|\sigma'(\xi)| \quad (10.18)$$

for $|n\sigma'(\xi)\epsilon| < 2$, or, $n\epsilon|\sigma'(\xi)|/2 < 1$. Let

$$N(\epsilon) = \left\lfloor \frac{2}{\epsilon|\sigma'(\xi(\epsilon))|} \right\rfloor \quad (10.19)$$

where $\lfloor \cdot \rfloor$ is the floor function ($\lfloor x \rfloor$: largest integer smaller than x). Then:

$$\left| \int_{x^*}^{x^*+\epsilon} \frac{\exp[in\sigma(x)]}{n} dx \right| \leq \frac{4\epsilon}{n} \left| \frac{\sigma'(\xi(\epsilon))}{\sigma'(x^*)} \right| \stackrel{\text{L10}}{<} \frac{6\epsilon}{n} \text{ for } n \leq N(\epsilon). \quad (10.20)$$

So now we have

$$\begin{aligned} & \left| \sum_{n=1}^{\infty} \int_{x^*}^{x^*+\epsilon} \frac{\exp[in\sigma(x)]}{n} dx \right| \leq \\ & \sum_{n=1}^{N(\epsilon)} \left| \int_{x^*}^{x^*+\epsilon} \frac{\exp[in\sigma(x)]}{n} dx \right| + \sum_{n=N(\epsilon)+1}^{\infty} \left| \int_{x^*}^{x^*+\epsilon} \frac{\exp[in\sigma(x)]}{n} dx \right| \leq \\ & \sum_{n=1}^{N(\epsilon)} \frac{6\epsilon}{n} + \sum_{n=N(\epsilon)+1}^{\infty} \frac{4}{n^2 |\sigma'(x^*)|}. \end{aligned} \quad (10.21)$$

Both sums vanish in the limit of $\epsilon \rightarrow 0$. We show this in the following way. For the first sum we obtain:

$$\sum_{n=1}^{N(\epsilon)} \frac{6\epsilon}{n} \stackrel{\text{L9}}{<} 6\epsilon[1 + \ln(N(\epsilon))] = 6\epsilon \left(1 + \ln \left\lfloor \frac{1}{\epsilon|\sigma'(\xi(\epsilon))|} \right\rfloor \right) <$$

$$6\epsilon \left\{ 1 - \ln(\epsilon) - \ln \left| \frac{\sigma'(\xi(\epsilon))}{\sigma'(x^*)} \right| - \ln |\sigma'(x^*)| \right\} <$$

$$6\epsilon \{1 - \ln(\epsilon) + \ln(2) - \ln |\sigma'(x^*)|\} \rightarrow 0 \text{ for } \epsilon \rightarrow 0. \quad (10.22)$$

For the second sum we obtain:

$$\sum_{n=N(\epsilon)+1}^{\infty} \frac{4}{n^2 |\sigma'(x^*)|} \stackrel{\text{L8}}{<} \frac{4}{|\sigma'(x^*)| N(\epsilon)} < \frac{12\epsilon}{4 - 3\epsilon |\sigma'(\xi(\epsilon))|} \rightarrow 0 \text{ for } \epsilon \rightarrow 0, \quad (10.23)$$

where we used

$$N(\epsilon) > \frac{2}{\epsilon |\sigma'(x^*)|} \left| \frac{\sigma'(x^*)}{\sigma'(\xi(\epsilon))} \right| - 1 \stackrel{\text{L10}}{>} \frac{4}{3\epsilon |\sigma'(x^*)|} - 1. \quad (10.24)$$

For the above proof we assumed $\sigma'(x^*) \neq 0$. But our proof still works for the case $\sigma'(x^*) = 0$ if we use $\sigma''(x)/\sigma''(x^*)$ instead of $\sigma'(x)/\sigma'(x^*)$ in (10.16). After a partial integration and noting that (i) $\lim_{\epsilon \rightarrow 0} \sigma'(x^* + \epsilon) = 0$ and (ii) $\forall |x - x^*| < \epsilon \exists C(\epsilon) > 0, \lim_{\epsilon \rightarrow 0} C(\epsilon) = 0 : [\sigma'(x)]^2 \leq C(\epsilon) |\sigma'(x)|$, we arrive at an equation very similar to (10.16). Then, following the steps (10.17) – (10.23) establishes T3 in this case too. This idea can be generalized to the case where the first non-vanishing derivative is of order n , i.e. $\sigma^{(k)}(x^*) = 0$ for $k = 0, 1, \dots, n - 1, \sigma^{(n)}(x^*) \neq 0$. In this case we use $\sigma^{(n)}(x)/\sigma^{(n)}(x^*)$ in (10.16). It is not possible that all derivatives of $\sigma(x)$ vanish at x^* since (making the physically justified assumption that $\sigma(x)$ is an entire function) this would mean that $\sigma(x)$ is identically zero and there exists a scattering channel in which “nothing happens”. Since these trivial scattering channels have no influence on the spectrum of a given quantum graph, it is possible to eliminate all trivial scattering channels and thus reduce the dimensionality of the S matrix such that none of the eigenphases of the new, reduced S matrix is constant. Taking this into account, our proof establishes T3 without any exceptions.

XI. APPENDIX B: FORMULAE, DEFINITIONS AND LEMMAS

This appendix is a collection of formulae, definitions and lemmas needed for the proofs presented in the text and in Appendix A. They are collected here since they are lowest in

the hierarchy of proof ideas. “Formulae” are identities that can be found in tables. We compiled them in this appendix for completeness and easy reference. “Lemmas” are simple theorems of a general nature that may be found in analysis text books, but are not usually easily accessible. So we compiled them here for completeness and convenience. “Theorems” are specific to the context of this paper. They are harder to prove and unlikely to be found in standard analysis text books. Every lemma and theorem is proved explicitly, unless a convenient proof is found in the literature (see, e.g., L11).

Formula F1: $1 - \cos(x) = 2 \sin^2(x/2)$.

Formula F2: (see [41] formula 1.4411, p. 44): $\sum_{\nu=1}^{\infty} \frac{\sin(\nu x)}{\nu} = \frac{\pi-x}{2}, \quad 0 < x < 2\pi$.

Formula F3: (see [41] formula 1.4412, p. 44): $\sum_{\nu=1}^{\infty} \frac{\cos(\nu x)}{\nu} = \frac{1}{2} \ln \left(\frac{1}{2[1-\cos(x)]} \right) \stackrel{F1}{=} -\ln(2) - \ln[\sin(x/2)], \quad 0 < x < 2\pi$.

Definition D1: A function f is differentiable in $x \iff \exists \lambda \in \mathbf{R} \forall \delta > 0 \exists \epsilon^*(\delta) > 0 \forall |\epsilon| < \epsilon^*$:

$$\left| \frac{f(x+\epsilon) - f(x)}{\epsilon} - \lambda \right| < \delta.$$

The constant λ is also denoted as $\lambda \equiv f'(x)$.

Lemma L1: Let $a, b \in \mathbf{R}$. Then: $|a + ib| = \sqrt{a^2 + b^2} \leq |a| + |b|$ (*).

Proof: $a^2 + b^2 \leq a^2 + 2|a||b| + b^2 = (|a| + |b|)^2$. Monotony of the square root yields (*).

Lemma L2: $1 - x^2/[n(n+1)] > 0$ for $|x| < 1$ and $n \in \mathbf{N}$.

Proof: $(|x|/n)(|x|/(n+1)) < 1 \Rightarrow 1 - x^2/[n(n+1)] > 0$.

Lemma L3: $|\sin(x)| \leq |x| \forall x \in \mathbf{R}$.

Proof: Trivial for $x = 0$ and $|x| \geq 1$. Let $|x| < 1$: $|\sin(x)| = \sin(|x|) = |x| - |x|^3[1 - x^2/(4 \cdot 5)]/3! - |x|^7[1 - x^2/(8 \cdot 9)]/7! - \dots \stackrel{L2}{\leq} |x|$.

Lemma L4: $|\sin(x)| \geq |x|/2$ for $|x| < 1$.

Proof: $|\sin(x)| = \sin(|x|) = |x|/2 + |x|(1 - x^2/3)/2 + |x|^5[1 - x^2/(6 \cdot 7)]/5! + \dots \stackrel{L2}{\geq} |x|/2$.

Lemma L5: $x^2/2 \leq |x|$ for $|x| \leq 2$.

Proof: $x \geq 0$: $x^2/2 - x = x(x-2)/2 \leq 0$ for $0 \leq x \leq 2$.

$x < 0$: $x^2/2 + x = x(x+2)/2 \leq 0$ for $-2 \leq x < 0$.

Lemma L6: $|\exp(ix) - 1| \leq 2|x|$ for $|x| \leq 2$.

Proof: $|\exp(ix) - 1| = |\cos(x) + i \sin(x) - 1| \stackrel{F1}{=} |-2 \sin^2(x/2) + i \sin(x)| \stackrel{L1}{\leq} 2 \sin^2(x/2) + |\sin(x)| \stackrel{L3}{\leq} 2(x/2)^2 + |x| \stackrel{L5}{\leq} 2|x|$ for $|x| \leq 2$.

Lemma L7: Let $f(x)$ be a monotonically decreasing function and $f(\nu) = a_\nu \in \mathbf{R}$, $\nu = 1, 2, \dots$. Let $M, N \in \mathbf{N}$, $M < N$. Then: $\sum_{\nu=M+1}^N a_\nu \leq \int_M^N f(x) dx$.

Proof: According to the intermediate value theorem of integral calculus $\exists \xi_\nu \in [\nu, \nu + 1]$ such that $\int_\nu^{\nu+1} f(x) dx = f(\xi_\nu)$. Then: $\int_M^N f(x) dx = \sum_{\nu=M}^{N-1} \int_\nu^{\nu+1} f(x) dx = \sum_{\nu=M}^{N-1} f(\xi_\nu) \geq \sum_{\nu=M}^{N-1} a_{\nu+1} = \sum_{M+1}^N a_\nu$.

Lemma L8: $\sum_{M+1}^\infty \frac{1}{n^\alpha} \leq \int_M^\infty \frac{1}{n^\alpha} dn = \frac{1}{(\alpha-1)M^{\alpha-1}}$ for $\alpha > 1$.

Proof: L7 with $N \rightarrow \infty$.

Lemma L9: $\sum_{n=1}^N \frac{1}{n} \leq 1 + \ln(N)$.

Proof: $\sum_{n=1}^N \frac{1}{n} = 1 + \sum_{n=2}^N \frac{1}{n} \stackrel{L7}{\leq} 1 + \int_1^N \frac{1}{n} dn = 1 + \ln(N)$.

Lemma L10: Let $f(x)$ be continuous in \mathbf{R} . Then: $\forall x^* \in \mathbf{R}$ with $f(x^*) \neq 0 \exists \epsilon^*(x^*) > 0 : 1/2 < f(x)/f(x^*) < 3/2 \quad \forall |x - x^*| < \epsilon^*(x^*)$ (#).

Proof: Since $f(x)$ is continuous: $\forall \delta \exists \epsilon(\delta) : |f(x) - f(x^*)| < \delta \quad \forall |x - x^*| < \epsilon(\delta)$. Choose $\delta = \delta^* := |f(x^*)|/2$ and define $\epsilon^* := \epsilon(\delta^*)$. Then: $|[f(x)/f(x^*)] - 1| < \delta^*/|f(x^*)| = 1/2 \quad \forall |x - x^*| < \epsilon^*$. This inequality can be used in two different ways: (i) $1 - f(x)/f(x^*) \leq |[f(x)/f(x^*)] - 1| < 1/2 \Rightarrow f(x)/f(x^*) > 1/2 \quad \forall |x - x^*| < \epsilon^*$. This is the first inequality in (#). (ii) $[f(x)/f(x^*)] - 1 \leq |[f(x)/f(x^*)] - 1| < 1/2 \Rightarrow f(x)/f(x^*) < 3/2 \quad \forall |x - x^*| < \epsilon^*$. This is the second inequality in (#).

Lemma L11: Let $\alpha_\nu, \beta_\nu \in \mathbf{R}$, $\nu = 1, 2, \dots$, $|\sum_{\nu=1}^\infty \alpha_\nu| < \infty$, $|\sum_{\nu=1}^\infty \beta_\nu| < \infty$, and $a, b \in \mathbf{R}$. Define: $S := \sum_{\nu=1}^\infty (a\alpha_\nu + b\beta_\nu)$. Then: $|S| < \infty$ and $S = a(\sum_{\nu=1}^\infty \alpha_\nu) + b(\sum_{\nu=1}^\infty \beta_\nu)$.

Proof: See [13], volume II, p. 3, theorem 1.2.1.

Lemma L12: $\sum_{\nu=1}^\infty \exp(i\nu x)/\nu$ exists and is finite in $0 < x < 2\pi$.

Proof: Follows immediately from F2, F3 and L11.

Lemma L13: Let $f(x)$ be differentiable in $x = a$ with $f(a) = a$ and $f'(a) < 1$. Then $\exists c > a$ with $c - f(c) > 0$.

Proof: Using D1 as the criterion for differentiability, we choose $\lambda = f'(a) < 1$, $\delta = 1 - \lambda$,

$0 < \gamma < \epsilon^*(\delta)$ and $c = a + \gamma$. Then:

$$\begin{aligned} \left| \frac{f(a + \gamma) - a}{\gamma} - \lambda \right| &\leq \left| \frac{f(a + \gamma) - f(a)}{\gamma} - \lambda \right| < \delta = 1 - \lambda. \\ \Rightarrow \left| \frac{f(a + \gamma) - a}{\gamma} \right| &< 1. \end{aligned}$$

Now:

$$c - f(c) = \gamma - \frac{f(a + \gamma) - a}{\gamma} \gamma \geq \gamma - \left| \frac{f(a + \gamma) - a}{\gamma} \right| \gamma > 0.$$

Lemma L14: Let $f(x)$ be differentiable in $x = a$ with $f(a) = a$ and $f'(a) < 1$. Then $\exists c < a$ with $f(c) - c > 0$.

Proof: Analogous to the proof of L13.

Lemma L15: Let $f(x)$ be continuous in $[a, b]$ with $f(a) = a$, $f(b) = b$, $f'(a) < 1$ and $f'(b) < 1$. Then there exists at least one additional fixed point z of f in $[a, b]$ with $a < z < b$.

Proof: Because of L13 there exists $c > a$ with $f(c) < c$. Because of L14 there exists $d < b$ with $f(d) > d$. Define $H(x) = f(x) - x$. Then $H(c) < 0$ and $H(d) > 0$. Since f is continuous, so is H . Then, because of the intermediate value theorem of calculus, $\exists z, a < c < z < d < b$, with $H(z) = 0$, i.e. $f(z) = z$.

Lemma L16: Let $f(x)$ be differentiable in $[a, b]$ with $f'(x) < 1 \forall x \in [a, b]$. Then f has at most one fixed point in $[a, b]$.

Proof: Assume that f has exactly $n > 1$ fixed points $x_1 < x_2 < \dots < x_n$ in $[a, b]$. Then, because of L15, there must be at least one additional fixed point between any pair of fixed points $x_j, j = 1, \dots, n$, bringing the total number of fixed points to at least $2n - 1 > n$, for $n > 1$. This contradicts the assumption that f has exactly $n > 1$ fixed points. Therefore f cannot have a finite number $n > 1$ of fixed points. Assume now that f has a countably infinite number of fixed points x_1, x_2, \dots in $[a, b]$. Then, according to Weierstraß, there exists an accumulation point x^* in $[a, b]$. This implies: $\forall \epsilon > 0 \exists x_n > x_m$ with $(x_n - x_m) < \epsilon$. Because f is differentiable we have according to D1:

$$\left| \frac{f(x_m + \epsilon) - f(x_m)}{\epsilon} - f'(x_m) \right| < \delta \quad \forall \epsilon < \epsilon^*(\delta). \quad (*)$$

Choose $\delta = 1 - f'(x_m)$, $0 < \epsilon = x_n - x_m < \epsilon^*(\delta)$, and use $f(x_n) = x_n$, $f(x_m) = x_m$, then

$$\left| \frac{f(x_m + \epsilon) - f(x_m)}{\epsilon} - f'(x_m) \right| = \left| \frac{f(x_n) - f(x_m)}{x_n - x_m} - f'(x_m) \right| = |1 - f'(x_m)| = 1 - f'(x_m) = \delta.$$

This contradicts equation (*). Therefore there cannot be a countably infinite number of fixed points in $[a, b]$. Now assume that f has a continuum of fixed points in $[a, b]$. In this case we can easily show that at an interior point x^* of the continuum of fixed points we have $f'(x^*) = 1$ in contradiction to $f'(x) < 1 \forall x \in [a, b]$. Therefore, in summary, there cannot be any finite number of fixed points $n > 1$, nor can there be infinitely many fixed points of f in $[a, b]$. The only alternatives are zero or one fixed point, i.e. at most one fixed point, as stated in L16.

Lemma L17: Let S be a unitary matrix of finite dimension $B \in \mathbf{N}$, $B \geq 1$. Denote by $\exp(i\sigma_1), \exp(i\sigma_2), \dots, \exp(i\sigma_B)$ its eigenvalues where $\sigma_j \in \mathbf{R}$ and $\sigma_j \bmod 2\pi \neq 0$. Define $M := \sum_{n=1}^{\infty} S^n/n$. Then: $|M_{ij}| < \infty$, $i, j = 1, \dots, B$.

Proof: Since S is unitary, there exists a unitary matrix Ω with $S = \Omega \text{diag}(\exp(i\sigma_1), \dots, \exp(i\sigma_B)) \Omega^\dagger$. Also: $S^n = \Omega \text{diag}(\exp(in\sigma_1), \dots, \exp(in\sigma_B)) \Omega^\dagger$. Define the series $\alpha^{(j)} = \sum_{n=1}^{\infty} \exp(in\sigma_j)/n$. According to L12 these series are convergent. Then, according to L11, $\mu_{jm} := \sum_{l=1}^B \Omega_{jl} \alpha^{(l)} \Omega_{ml}^*$ is convergent, and therefore finite, because only a finite sum over $\alpha^{(l)}$ is involved. Again with L11: $\mu_{jm} = \sum_{n=1}^{\infty} (1/n) \sum_{l=1}^B \Omega_{jl} \exp(in\sigma_l) \Omega_{ml}^* = \sum_{n=1}^{\infty} (1/n) (S^n)_{jm} = M_{jm}$. This means that since μ_{ij} is finite, so is M_{ij} , i.e. $|M_{ij}| < \infty$.

Lemma L18: Let S be the matrix of L17. Then: for $0 < \sigma_j < 2\pi$, $j = 1, \dots, B$: $\text{Tr} \sum_{n=1}^{\infty} S^n/n = \sum_{j=1}^B \{-\ln(2) - \ln[\sin(\sigma_j/2)] + i(\pi - \sigma_j)/2\}$.

Proof: Because of L11,

$$\begin{aligned} \text{Tr} \sum_{n=1}^{\infty} \frac{1}{n} S^n &= \sum_{n=1}^{\infty} \frac{1}{n} \text{Tr} S^n = \sum_{n=1}^{\infty} \frac{1}{n} \text{Tr} \{ \Omega \text{diag}[\exp(in\sigma_1), \dots, \exp(in\sigma_B)] \Omega^\dagger \} = \\ &= \sum_{n=1}^{\infty} \frac{1}{n} [\exp(in\sigma_1) + \dots + \exp(in\sigma_B)] \stackrel{\text{F2, F3, L11}}{=} \sum_{j=1}^B \{-\ln(2) - \ln[\sin(\sigma_j/2)] + i(\pi - \sigma_j)/2\}. \end{aligned}$$

Lemma L19: $\text{Im} \text{Tr} \sum_{n=1}^{\infty} S^n/n = \sum_{j=1}^B (\pi - \sigma_j)/2$.

Proof: Follows immediately from L18.

Lemma L20: $\ln |\sin(x)|$ has an integrable singularity at $x = 0$.

Proof: Let $b < \pi/2$. Then:

$$\left| \int_0^b \ln[\sin(x)] dx \right| \stackrel{\text{L4}}{\leq} \left| \int_0^b \ln(x/2) dx \right| = b |\ln(b/2) - 1| < \infty.$$

REFERENCES

- [1] R. L. Devaney, *A First Course in Chaotic Dynamical Systems* (Addison-Wesley Publishing Company, Inc., Reading, Massachusetts, 1992).
- [2] E. Ott, *Chaos in Dynamical Systems* (Cambridge University Press, Cambridge, 1993).
- [3] R. M. May, in *Dynamical Chaos*, M. V. Berry, I. C. Percival, and N. O. Weiss, editors (Princeton University Press, Princeton, New Jersey, 1987), p. 27.
- [4] S. M. Ulam and J. von Neumann, *Bull. Am. Math. Soc.* **53**, 1120 (1947).
- [5] R. Blümel and W. P. Reinhardt, *Chaos in Atomic Physics* (Cambridge University Press, Cambridge, 1997).
- [6] M. Gutzwiller, *Chaos in Classical and Quantum Mechanics* (Springer, New York, 1990).
- [7] H.-J. Stöckmann, *Quantum Chaos* (Cambridge University Press, Cambridge, 1999).
- [8] R. Blümel, Yu. Dabaghian, and R. V. Jensen, *Phys. Rev. Lett.* **88**, 044101 (2002).
- [9] Y. Dabaghian, R. V. Jensen, and R. Blümel, *Phys. Rev. E* **63**, 066201 (2001).
- [10] R. Blümel, Yu. Dabaghian, and R. V. Jensen, *Phys. Rev. E*, in press (2002).
- [11] Yu. Dabaghian, R. V. Jensen, and R. Blümel, *Pis'ma v ZhETF* **74**, 258 (2001); *JETP Lett.* **74**, 235 (2001).
- [12] Yu. Dabaghian, R. V. Jensen, and R. Blümel, *JETP*, in press (2002).
- [13] K. Endl and W. Luh, *Analysis*, three volumes (Akademische Verlagsgesellschaft, Frankfurt am Main, 1972).
- [14] A. S. Demidov, *Generalized Functions in Mathematical Physics* (Nova Science Publishers, Huntington, 2001).
- [15] W. Walter, *Einführung in die Theorie der Distributionen* (Bibliographisches Institut, Mannheim, 1974).

- [16] P. A. M. Dirac, *The Principles of Quantum Mechanics*, fourth edition (Oxford University Press, Oxford, 1958).
- [17] J. von Neumann, *Mathematical Foundations of Quantum Mechanics* (Princeton University Press, Princeton, 1955).
- [18] T. Kottos and U. Smilansky, Phys. Rev. Lett. **79**, 4794 (1997); Ann. Phys. (N.Y.) **274**, 76 (1999).
- [19] S. P. Novikov, Usp. Math. Nauk, **52 (6)**, 177 (1997).
- [20] S. P. Novikov and I. A. Dynnykov, Usp. Math. Nauk **52(5)**, 175 (1997).
- [21] K. Rudenberg and C. Scherr, J. Chem. Phys. **21**, 1565 (1953).
- [22] E. Akkermans, A. Comtet, J. Desbois, G. Montambaux, and C. Texier, Ann. Phys. (N.Y.) **284**, 10 (2000).
- [23] Proceedings of the International Conference on *Mesoscopic and Strongly Correlated Electron Systems "Chernogolovka 97"*, chapter 4: *Quasi-1D Systems, Networks and Arrays*, edited by V. F. Gantmakher and M. V. Feigel'man, Usp. Fiz. Nauk **168**, pp. 167–189 (1998).
- [24] H. Schanz and U. Smilansky, Phys. Rev. Lett. **84**, 1427 (2000); Philos. Mag. B **80**, 1999 (2000).
- [25] U. Smilansky, J. Phys. A (Mathematical and General) **33**, 2299 (2000).
- [26] F. Barra and P. Gaspard, J. Stat. Phys. **101**, 283 (2000); Phys. Rev. E **65**, 016205 (2002).
- [27] P. Pakonski, K. Zyczkowski, and M. Kus, J. Phys. A (Mathematical and General) **34**, 9303 (2001).
- [28] U. Smilansky, in *Mesoscopic Quantum Physics*, Les Houches, Session LXI, 1994, edited

- by E. Akkermans, G. Montambaux, J.-L. Pichard and J. Zinn-Justin (Elsevier Science Publishers, Amsterdam, 1995), pp. 373–433.
- [29] R. Blümel and Yu. Dabaghian, *J. Math. Phys.* **42**, 5832 (2001).
- [30] Y.-C. Lai, C. Grebogi, R. Blümel, and M. Ding, *Phys. Rev. A* **45**, 8284 (1992).
- [31] L. Sirko, P.M. Koch, and R. Blümel, *Phys. Rev. Lett.* **78**, 2940 (1997).
- [32] Sz. Bauch, A. Błędowski, L. Sirko, P.M. Koch, and R. Blümel, *Phys. Rev. E* **57**, 304 (1998).
- [33] R. Blümel, P. M. Koch, and L. Sirko, *Found. Phys.* **31**, 269 (2001).
- [34] M. Keeler and T. J. Morgan, *Phys. Rev. Lett.* **80**, 5726 (1998).
- [35] A. C. Aitken, *Determinanten und Matrizen* (Bibliographisches Institut AG, Mannheim, 1969).
- [36] R. Courant, *Differential and Integral Calculus*, second edition, two volumes (Interscience Publishers, New York, 1937).
- [37] R. Courant and D. Hilbert, *Methods of Mathematical Physics*, first English edition, two volumes (Interscience Publishers, New York, 1953).
- [38] J. H. van Lint and R. M. Wilson, *A Course in Combinatorics* (Cambridge University Press, Cambridge, 1992).
- [39] J. Riordan, *An Introduction to Combinatorial Analysis* (Wiley, New York, 1958).
- [40] *Handbook of Mathematical Functions*, edited by M. Abramowitz and I. A. Stegun (National Bureau of Standards, Washington D.C., 1964).
- [41] I. S. Gradshteyn and I. M. Ryzhik, *Table of Integrals, Series, and Products*, 6th edition, A. Jeffrey, Editor, D. Zwillinger, Assoc. Editor (Academic Press, San Diego, 2000).
- [42] G. Sansone and H. Gerretsen, *Lectures on the Theory of Functions of a Complex Variable*

(Noordhoff, Groningen, 1960).

- [43] T. Kottos and H. Schanz, *Physica E* **9**, 523 (2001).
- [44] F. Haake, *Quantum Signatures of Chaos* (Springer, Berlin, 1991).
- [45] E. B. Bogomolny, B. Georgeot, M.-J. Giannoni, and C. Schmit, *Phys. Rev. Lett.* **69**, 1477 (1992).
- [46] H. Bohr, *Almost Periodic Functions* (Chelsea Publishing, New York, 1951).
- [47] B. J. Lewin, *Nullstellenverteilung ganzer Funktionen* (Akademie-Verlag, Berlin, 1962).
- [48] L. I. Schiff, *Quantum Mechanics*, second edition (McGraw-Hill, New York, 1955), p. 37.
- [49] A. Messiah, *Quantenmechanik*, volume I (Walter de Gruyter, Berlin, 1976), p. 89.

Figure Captions

Fig. 1: Sketch of a quantum graph with six vertices and ten bonds.

Fig. 2: Structure of root cell I_n . To the left and to the right of I_n are the root-free intervals $F_n^{(-)}$ and $F_n^{(+)}$, respectively. Together they form the root-free zone $F_n = F_n^{(-)} \cup F_n^{(+)}$. Roots of the spectral equation are found in the interval R_n . The delimiters of I_n are \hat{k}_{n-1} and \hat{k}_n . The average location (star) of the root k_n is given by \bar{k}_n .

Fig. 3: Graphical solution of the spectral equation $\cos(x) = \Phi(x)$. Since $\cos(x)$ is “faster” than $\Phi(x)$, one and only one solution exists in every interval $(n\pi, (n+1)\pi)$. This fact is proved rigorously in Sec. III.

Fig. 4: Detail of the spectral staircase illustrating the computation of the integral (4.5) over the spectral staircase from \hat{k}_{n-1} to k_n for the purpose of obtaining an explicit expression for k_n .

Fig. 5: Three-vertex linear quantum graph. The vertices are denoted by V_1 , V_2 and V_3 , respectively. V_1 and V_3 are “dead-end” vertices. The bonds are denoted by B_{12} and B_{23} , respectively. While there is no potential on the bond B_{12} (indicated by the thin line representing the potential-free bond B_{12}), the bond B_{23} is “dressed” with the energy-dependent scaling potential $U_{23} = \lambda E$ (indicated by the heavy line representing the “dressed” bond B_{23}).

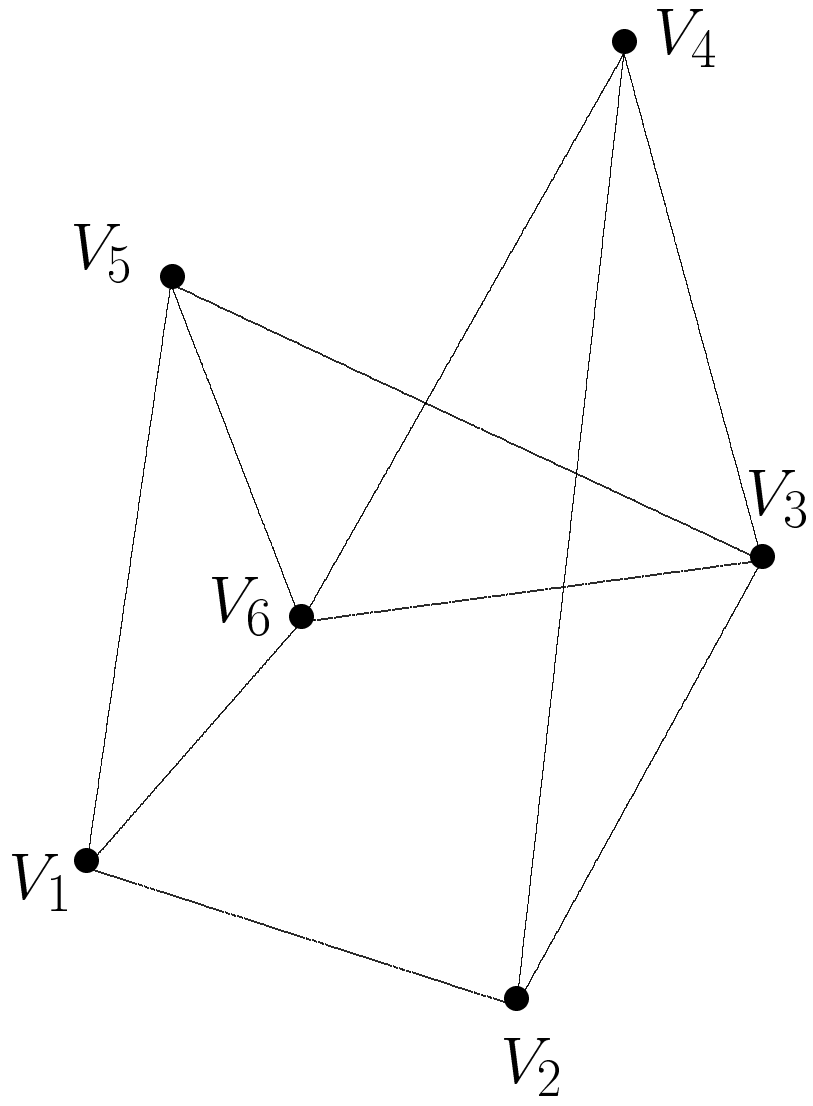


Fig. 1

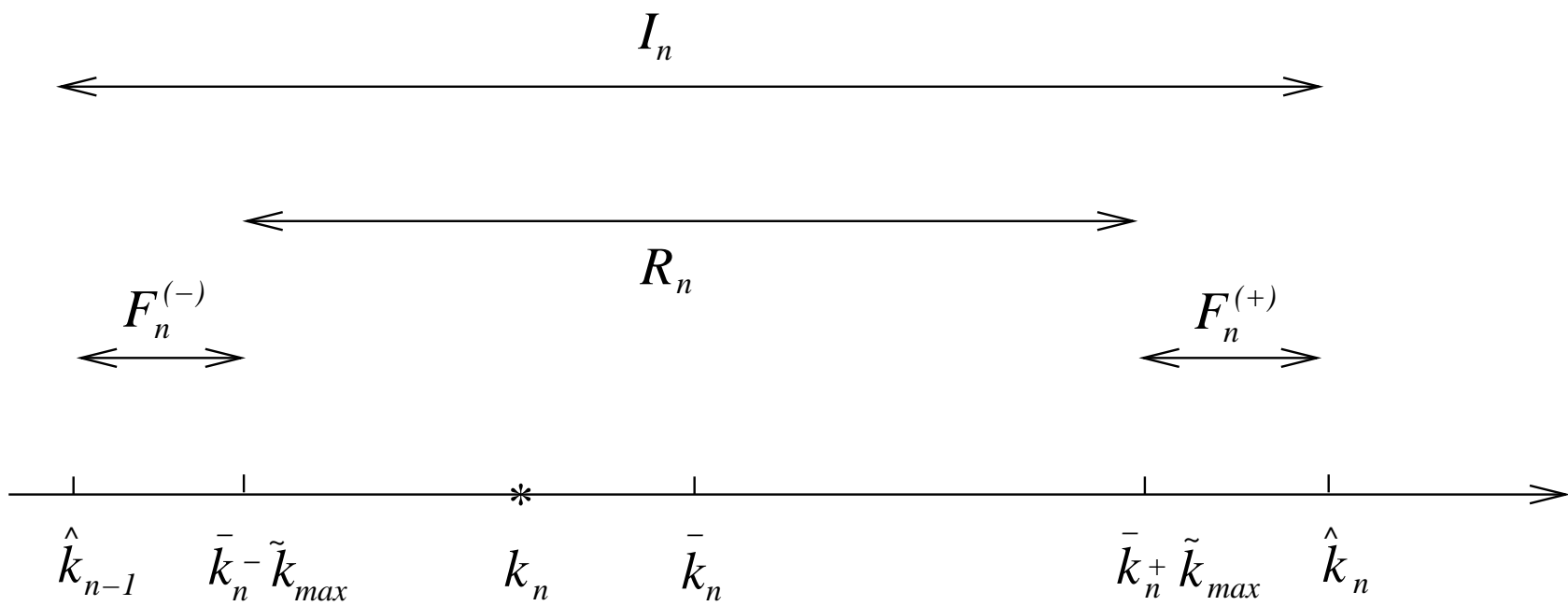


Fig. 2

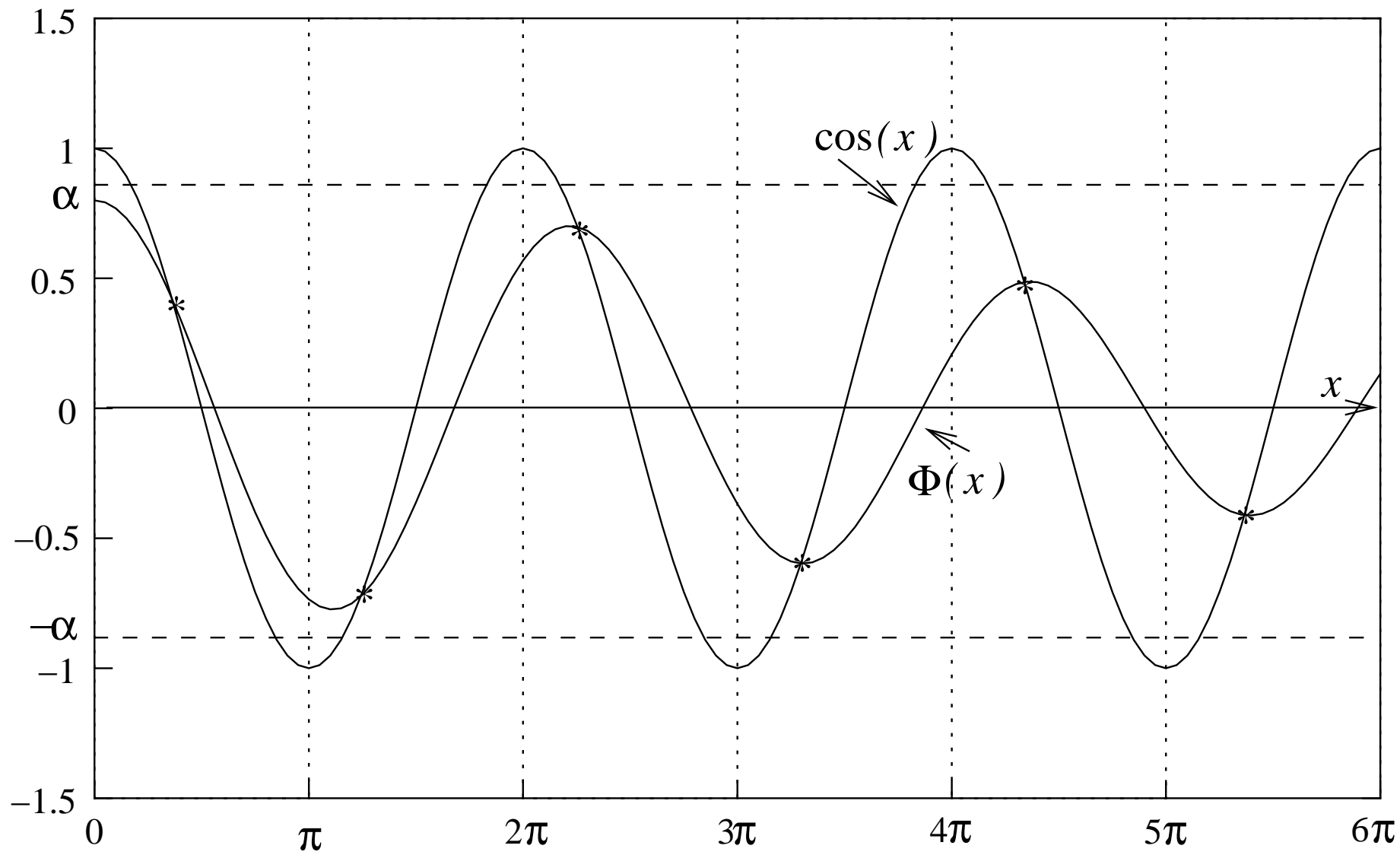


Fig. 3

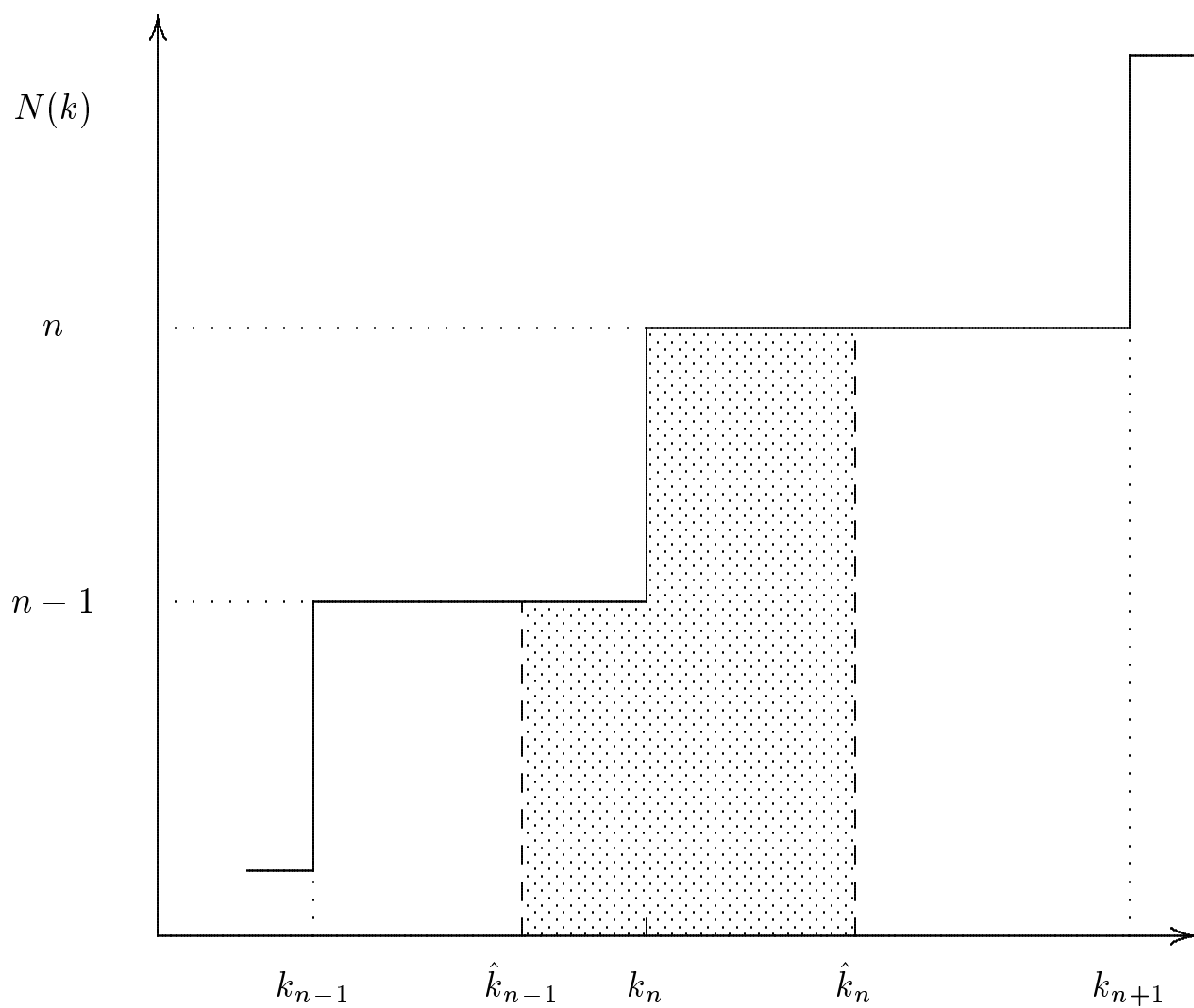


Fig.4

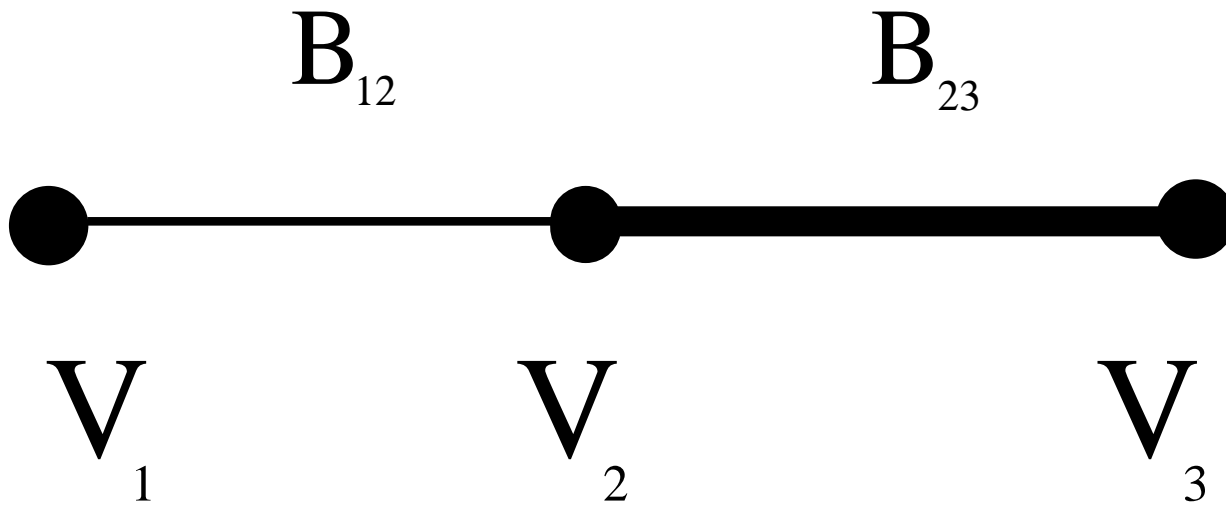


Fig. 5